



*Advanced Nuclear Technology Group NEN-2  
Nuclear Engineering and Nonproliferation Division*

*W.F.M.*  
**To:** William Myers, NEN-2, MS B228  
**From:** George McKenzie, NEN-2, B228 GEM  
**Phone:** 505-606-0034  
**Symbol:** NEN-2: 18-033  
LA-UR-18-27548  
**Date:** June 11, 2018

**Subject: NCSP Foreign Trip Report for George McKenzie, Physor 2018 Cancun, MX**

The trip to the Physor 2018 conference was an excellent career development opportunity. I was able to present my dissertation work which consisted of NCSP funded measurements. The summary that was published in the conference proceedings was entitled "Subcritical Reactivity Determination using Rossi- $\alpha$  Measurements on a Thermal System<sup>1</sup>". Similarly the oral presentation given during the conference was entitled "Limits on Subcritical Reactivity Determination Using Rossi- $\alpha$  and Related Methods<sup>2</sup>". Both references are attached, respectively, as APPENDIX A and APPENDIX B. In addition to my presentation, I was also able to attend many other interesting talks to learn about experiments, methods, and simulation tools capable of improving future work. This conference included several talks by about ICSBEP and IRPhE benchmarks including a plenary overview of OECD given by Tatiana Ivanova.

The conference also provided the opportunity to conduct side conversations with several collaborators from organizations such as CEA, IRSN, MIT, and other universities. This collaboration will prove beneficial to the work I am able to produce for the NCSP program.

Best,

George McKenzie

---

<sup>1</sup> G. McKenzie, et. al., "Subcritical Reactivity Determination using Rossi- $\alpha$  Measurements on a Thermal System," Los Alamos National Laboratory report LA-UR-17-29783, (2017).

<sup>2</sup> G. Mckenzie, "Limits on Subcritical Reactivity Determination Using Rossi- $\alpha$  and Related Methods", Los Alamos National Laboratory report LA-UR-18-21131, (2018).

## **APPENDIX A**

# SUBCRITICAL REACTIVITY DETERMINATION USING ROSSI- $\alpha$ MEASUREMENTS ON A THERMAL HEU SYSTEM

G. McKenzie<sup>1\*</sup>, T. Grove<sup>1</sup>, R. Sanchez<sup>1</sup>, and W. Myers<sup>1</sup>

<sup>1</sup>Los Alamos National Laboratory  
PO Box 1663 Los Alamos, NM 87545

gmckenzie@lanl.gov

## ABSTRACT

The measurement of subcritical reactivity has become an expanding area of research in the past several years. Most of this interest is due to the desire to build accelerator driven reactor systems that operate below critical using the neutron multiplication from the system to increase the total neutron flux from the accelerator. Reactivity worth for operating reactor systems is measured by comparing to a known critical configuration. The flaw to worth measurements is that only measurements near critical are accurate. For many subcritical techniques, a measurement of multiplication is made as the configuration changes to become closer to critical. Most subcritical measurement techniques have their own flaw. As the multiplication grows as the system nears critical, the associated uncertainty rapidly increases. The Rossi- $\alpha$  measurement technique discussed in this paper works well near critical, and this paper attempts to examine the extent of its applicability in the subcritical regime. This may prove interesting as the Rossi- $\alpha$  technique is not affected by the amount of total excess reactivity in a system. Using the Rossi- $\alpha$  technique, subcritical reactivity has been determined using linear extrapolation if the value of  $\alpha$  at critical is known. This method has been well proven near delayed critical,  $0.98 < k_{eff} \leq 1$ . This study experimentally determines  $\alpha$  for a thermal system of Polyethylene and HEU. This type of system is often used to represent a solution system. The Rossi- $\alpha$  measurements discussed cover an effective multiplication factor range between  $0.64 \leq k_{eff} \leq 1$ . Calculations are also performed to compare to experimental cases, and to extend the work beyond the experimental data presented here. As predicted, the linear relationship between  $\alpha$  and reactivity no longer holds true for  $k_{eff} \lesssim 0.85$ .

KEYWORDS: Rossi- $\alpha$ , Subcritical, HEU, Prompt Neutron Decay Constants

## 1. INTRODUCTION

Since the 1940s, the Rossi- $\alpha$  measurement technique has been used to determine the neutron lifetime of chain-reacting nuclear systems [1]. Through examination of the definition of  $\alpha$  it was also

---

\*Corresponding Author

apparent that  $\alpha$  would scale linearly with reactivity near delayed critical [2,3]. This allows subcritical reactivity to be determined using linear extrapolation. The Rossi- $\alpha$  technique is derived using the point reactor kinetics model. Therefore, the assumptions of point reactor kinetics must be adhered to for the model to be valid. When this work initiated several years ago, the original goal was to measure the breakdown of point reactor kinetics assumptions with respect to the relationship between  $\alpha$  and reactivity. The original intention of the work used Godiva IV which is a fast system. This goal has since changed due to the hardware challenges related to measuring such a quantity in a fast system. Simultaneous to the issues encountered by this project a paper was written by Klain discussing the measurement system requirements to measure Rossi- $\alpha$  on highly subcritical fast metal systems [4]. This work examines a benchmarked, thermal critical experiment to determine where the point kinetics model breaks down and no longer allows a linear extrapolation to the subcritical reactivity of a chain-reacting system.

## **2. ROSSI- $\alpha$ THEORY**

The prompt neutron decay constant, often referred to as the Rossi- $\alpha$  or  $\alpha$ -eigenvalue, is a dynamic variable of a chain-reacting nuclear fission system. The prompt neutron decay constant of a system is a measure of how quickly the prompt neutron population changes as a function of time. The time behavior of the prompt neutron population is modeled well by an equation developed by Richard Feynman congruently with Rossi's development of his experiment [1]. Like the Inhour relation,  $\alpha$ -eigenvalue methods are another useful method of calibrating reactivity [5–8], as long as the value of  $\alpha$  at delayed critical is well defined. For systems at delayed critical, this measurement directly provides the  $\alpha$ -eigenvalue for the system, but when a system is not at delayed critical the value measured can be used to infer the  $\alpha$ -eigenvalue of a system. Measurements of the  $\alpha$ -eigenvalue rely on a certain set of assumptions to be valid. The first and most important assumption is that the system is in a fundamental mode without significant fission chain overlap [8,9]. The second assumption is that the measurement is taken at a point that is symmetric with respect to source and detector geometry, so that spatial considerations do not need to be considered [10]. The third and final assumption is that the system is not heavily reflected [7].

An understanding of the distinction between accidental and correlated neutron pairs is crucial to the comprehension of how  $\alpha$ -eigenvalue methods were developed. Much like the distinction between prompt and delayed neutrons, dividing the detected neutrons into two groups is necessary to complete the analysis of the prompt neutron decay constant. In a single fission chain, the accidental and correlated neutron pairs relate to the prompt and delayed neutron groups. Correlated neutrons refer to the prompt neutrons generated from a common fission ancestor. Accidental neutrons are defined to be neutrons originating from a random source such as the background or delayed emission. When multiple fission chains are being analyzed, neutrons originating in a different fission chain are considered as accidental neutron pairs.

A visual representation of accidental and correlated neutron pairs is provided in Fig. 1. In Fig. 1, X is the common fission ancestor to correlated neutron pairs like C, D, and G. Correlated neutron pairs are also seen in the other chains at A and E or B and F. Any combination of neutrons from separate chains denotes accidental neutron pairs, such as A and B.

The Rossi- $\alpha$  method measures the correlation in neutron counts to determine  $\alpha$ . Rossi proposed that active fission systems are self-modulated; meaning that the emission rate of delayed neutrons is

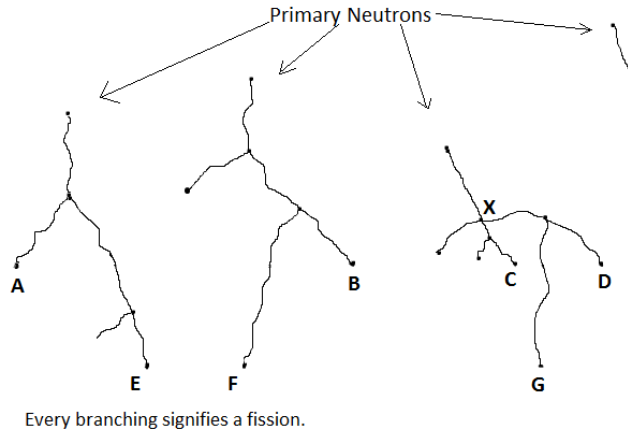


**Figure 1: Visual Representation of Accidental and Correlated Neutron Pairs [11].**

sufficiently slow that neutrons produced directly from two separated fission events are discernible [12]. The prompt neutron decay constant,  $\alpha$ , depends on both the prompt multiplication factor,  $k_p$ , and the neutron lifetime,  $l$ , which is defined as the time for one prompt neutron to be removed from the neutron multiplying system [13]. Specifically, the prompt neutron lifetime is the average length of time a prompt neutron exists in a system before a terminating event. Termination can be caused by leakage from the system, non-fission capture, or fission capture.

Experiments using the Rossi- $\alpha$  method are performed subprompt critical. Measurements of  $\alpha$  between delayed and prompt critical are often difficult because the power level and subsequently the neutron population of the neutron multiplying system are increasing. The increasing neutron population poses two issues to Rossi- $\alpha$  measurements. The first issue is the saturation of the detection system. The second issue is the increasing overlap of fission chains. Although the methods described are not valid, measuring  $\alpha$  above prompt critical is possible by measuring the prompt period of the neutron multiplying system. Above prompt critical,  $\alpha$  is defined as the inverse of the prompt period, as delayed neutrons are born too slowly to affect measurements in this regime.

To understand Feynman's derivation of the prompt neutron population in a neutron multiplying system, imagine the first fission in a chain reacting system occurring at some time  $t_0$ . This fission emits several neutrons during the fission process. One of these neutrons survives to cause another fission which in turn emits several neutrons. This neutron chain eventually generates a fission where one neutron is detected by our detector, at some time  $t_1$ , and a separate neutron generates another fission. At some time  $t_2$ , the detection system detects another neutron. The detection event at  $t_2$  is either correlated to the event detected at  $t_1$ , or it has no correlation to the detection event at  $t_1$  and is considered accidental. Using the statistics of the likelihood of this sequence of events, a distribution of the promptly born neutron population as a function of time is created. This process is completed over and over again until the distribution smooths and the distribution can be described by a single expression. When a system is subprompt, the prompt neutron population decays as a function of time because the likelihood of prompt neutron in any given chain surviving is low. Thus, all chains decay back to some constant background determined by the random neutron

population at the time of the measurement. This background is related to the strength of the interrogating source, and the multiplication of the system. The multiplication of the system is important because delayed neutrons are born randomly in time, and are therefore treated as a random source of neutrons.

The probability that a fission occurs at time  $t_0 = 0$  can be generalized by Eq. 1 to be equal to the average fission rate,  $F$ .

$$p_0(t_0)\Delta_0 = F\Delta_0 \quad (1)$$

In general,  $p_x$  is the probability of detecting a neutron count number  $x$  at a time  $t_x$ . The time  $t_x$  exists within the time window  $\Delta_x$ .

The probability of another neutron due to fission being detected at some  $t_1$  after the initial count, which occurred at  $t_0$ , is of interest. The probability of this second neutron being detected can be quantified by Eq. 2.

$$p_1(t_1)\Delta_1 = \epsilon\nu_p v \Sigma_f e^{\alpha(t_1-t_0)} \Delta_1 \quad (2)$$

In Eq. 2,  $\epsilon$  is the efficiency of the detector in counts per fission,  $\nu_p$  is the number of prompt neutrons emitted,  $v$  is the velocity of thermal neutrons, and  $\Sigma_f$  is the macroscopic fission cross section. When the terms  $v$  and  $\Sigma_f$  are combined they become the average fission rate per unit neutron density  $v\Sigma_f$  [7].

Next, the probability of a neutron count occurring at time  $t_2$  after detection events occurred at both  $t_0$  and at  $t_1$  and from the same fission chain is of interest. The probability is quantified in Eq. 3.

$$p_2(t_2)\Delta_2 = \epsilon(\nu_p - 1)v\Sigma_f e^{\alpha(t_2-t_0)} \Delta_2 \quad (3)$$

Notice that the  $\nu$  term has been modified to  $(\nu - 1)$  to account for the neutron lost at  $t_1$  in the fission chain [7].

All three of the probabilities calculated in Eq. 1, Eq. 2, and Eq. 3 are independent and can be joined to give the probability of occurrence of two chain-related, correlated ( $p_c$ ) counts initiated by a fission at time  $t_0$ ; the first subsequent count occurring at time  $t_1$  in  $\Delta_1$  and the second happening at some time  $t_2$  in  $\Delta_2$  [7]. The probability of the above-mentioned sequence occurring can be found by integrating the product of the probabilities for events at  $t_1$  and  $t_2$  over all time up until  $t_1$ . This integration is performed because there is no way to know that a detected count is caused directly from the fission. Instead, it is assumed that detected neutrons relate to the detection events at time  $t_1$  and  $t_2$ . Eq. 4 portrays the probability of two chain related events occurring as a result of a fission at time  $t_0$ .

$$p_c(t_1, t_2)\Delta_1\Delta_2 = F\epsilon^2 \frac{D_\nu k_p^2}{2(1 - k_p)l} e^{\alpha(t_2-t_1)} \Delta_1\Delta_2 \quad (4)$$

Eq. 4 is additionally simplified using  $\overline{\nu_p(\nu_p - 1)}$  as an average of the number of prompt neutrons emitted and the identities shown in Eq. 5 and Eq. 6.

$$\overline{\nu_p} = \frac{k_p \Sigma_a}{\Sigma_f} = \frac{k_p}{\Sigma_f v l} \quad (5)$$

$$D_\nu = \frac{\overline{\nu_p(\nu_p - 1)}}{\nu_p^2} \quad (6)$$

These identities refer to the definitions of the average emission of prompt neutrons and Diven's parameter,  $D_\nu$ , respectively [7]. Diven's parameter accounts for the dispersion of the neutron emission [11,14,15]. Diven's parameter is a cleaner way of representing the information originally derived by Feynman [1].

Accidental pairs have constant rate with respect to time and are thus represented as a constant probability. The probability that the counts seen at time  $t_1$  and  $t_2$  are an accidental pair is the same as the product of the average fission rate and the efficiency of the detector in the time bin. This probability can be seen in Eq. 7 [7,8,3].

$$p_r(t_1, t_2)\Delta_1\Delta_2 = F^2\epsilon^2\Delta_1\Delta_2 \quad (7)$$

The total probability for observing a pair of counts in  $\Delta_1$  and  $\Delta_2$  is the aggregate of the probabilities found above as shown in Eq. 8 [7]. The Rossi experiment guarantees an interaction in the time interval  $\Delta_1$  because the interaction at  $t_1$  is the initiating event. With some manipulation, the probability of the first count occurring in the time interval  $\Delta_1$ ,  $F\epsilon\Delta_1$ , can be separated and set to 1 as shown by Eq. 8 [7].

$$p(t)\Delta = F\epsilon\Delta + \epsilon\frac{D_\nu k_p^2}{2(1-k_p)l}e^{\alpha t}\Delta \quad (8)$$

The exponential including  $\alpha$  has been shown here with a positive sign. The prompt neutron decay constant has been modeled using many different sign conventions. The sign conventions used in this paper follow the sign conventions used by Orndoff [3]. Orndoff's convention defines  $\alpha$  to be negative when below prompt critical.

Often, for simplicity, the total probability to detect a neutron event in some  $\Delta_2$  after detecting an event at  $\Delta_1$  is written in the general form shown in Eq. 9. Eq. 9 is fit to experimental data during analysis.

$$P(t) = A + Be^{\alpha t} \quad (9)$$

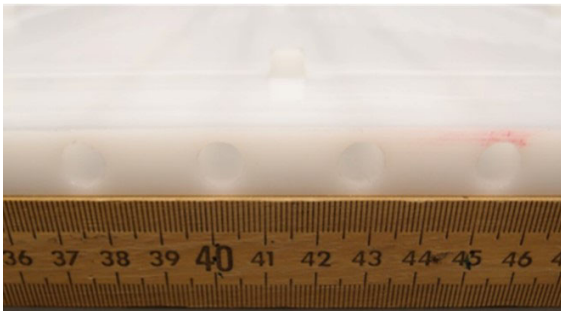
### 3. RESULTS

The Class Foils experiment with polyethylene interstitial plates is one of the tools used to teach criticality safety at the National Criticality Experiments Research Center (NCERC). This set of polyethylene plates is designed to provide the optimal H/ $^{235}\text{U}$  ratio on the critical mass curve allowing the experiment to have the minimum amount of  $^{235}\text{U}$  [16]. This experiment is a great teaching tool demonstrating that changing the  $^{235}\text{U}$  mass or amount of moderation affects the critical mass [16]. For this experiment, adding additional mass or additional moderation increases the critical mass. This effect is possible because of the optimal ratio between H/ $^{235}\text{U}$ ; with either change shifting the "effective" concentration of  $^{235}\text{U}$  in the assembly.

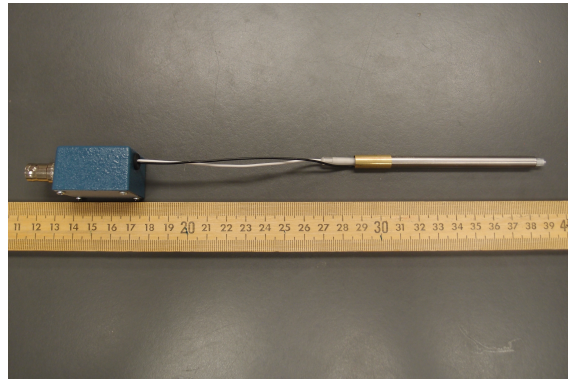
This experiment has been historically performed using either polyethylene or Lucite interstitial moderating plates. The increased hydrogen density of polyethylene compared to the Lucite plates has reduced the critical mass for the polyethylene moderated experiment by 34%. The critical mass of the Class Foils experiment using polyethylene interstitial is  $997.9 \pm 0.65$  g [16]. The fuel foils consist of thin highly enriched uranium (93 wt%  $^{235}\text{U}$ ) metal foils laminated in plastic; each foil weighs approximately 68 grams. The fuel is interleaved between interstitial polyethylene plates to

6		1"
4B Poly		1"
4C Poly		1"
2N Poly	10C HEU	0.5"
2M Poly	11C HEU	0.5"
2H Poly	12C HEU	0.5"
2G Poly	13C HEU	0.5"
2E Poly	14C HEU	0.5"
10 RTD	15C HEU	0.5"
Rossi Alpha Plate	16C HEU	0.5"
3 Membrane Poly	17C HEU	0.5"
2C Poly	18C HEU	0.5"
2I Poly	19C HEU	0.5"
2J Poly	20C HEU	0.5"
2K Poly	21C HEU	0.5"
2L Poly	22C HEU	0.5"
2F Poly	23C HEU	0.5"
2D Poly	24C HEU	0.5"
9 Poly Source	25C HEU	0.5"
11 Poly		0.5"
4A Poly		1"
5 Poly		1"

**Figure 2: Critical Configuration of the Class Foils Experiment with the Specially Modified Plate and Detection System.**



(a) Holes in Specially Designed Plate.



(b)  $^3\text{He}$  Detector used in the Experiment.

**Figure 3: Additional Equipment added to the Class Foils for the Rossi- $\alpha$  Experiments.**

attain a critical configuration. The system is shown in Fig. 2. The critical configuration requires 14.5 fuel foils.

Discussed in this section are the results of both the experiments and the calculations performed using the Rossi- $\alpha$  method on the Class Foils Experiment.

### 3.1. Experimental Results

For the Rossi- $\alpha$  experiment, a special moderator plate was designed to hold four detectors. The plate is shown in Fig 3a. This plate could theoretically be placed at any location in the stack. As a good practice, the special plate has been located only on the stationary half of the assembly during remote operations.

Rossi- $\alpha$  measurements can be performed with a wide range of neutron detectors. Helium-3 ( $^3\text{He}$ ) detectors were selected in this case. The detectors are manufactured by Reuter-Stokes (RS-P4-0203-201), with a 0.25" inch diameter, an active length of approximately 3" inches, and a  $^3\text{He}$  pressure of 40 atm [17,18]. One of the  $^3\text{He}$  detectors is shown in Fig. 3b.

The addition of the Rossi- $\alpha$  experimental equipment has added significant negative reactivity worth due to the absorption properties of the detectors. As such, additional fuel plates were added to counteract the negative reactivity worth. The critical configuration with the detection system consists of 16 units when the detectors are centered in the assembly. The critical configuration with the special modified plate and detectors is shown in Figs. 2 and 4.

The experiment was performed using two methods of reducing reactivity. The first method was to use separation of the two halves using the assembly to adjust reactivity. The experiments performed as a function of separation were used to derive the value of  $\alpha$  at delayed critical which can also be referred to as the  $\alpha$ -eigenvalue. Measurements were taken at 34, 63, and 94 mils below critical. The  $\alpha$ -eigenvalue determined for the Polyethylene Class Foils Experiment is  $-199.2s^{-1}$ . The  $\alpha$ -eigenvalue is derived based on fitting a line to a plot of  $\alpha$  versus the inverse count rate. The y-intercept of this linear fit is the  $\alpha$ -eigenvalue. For the Polyethylene Class Foils, this result is

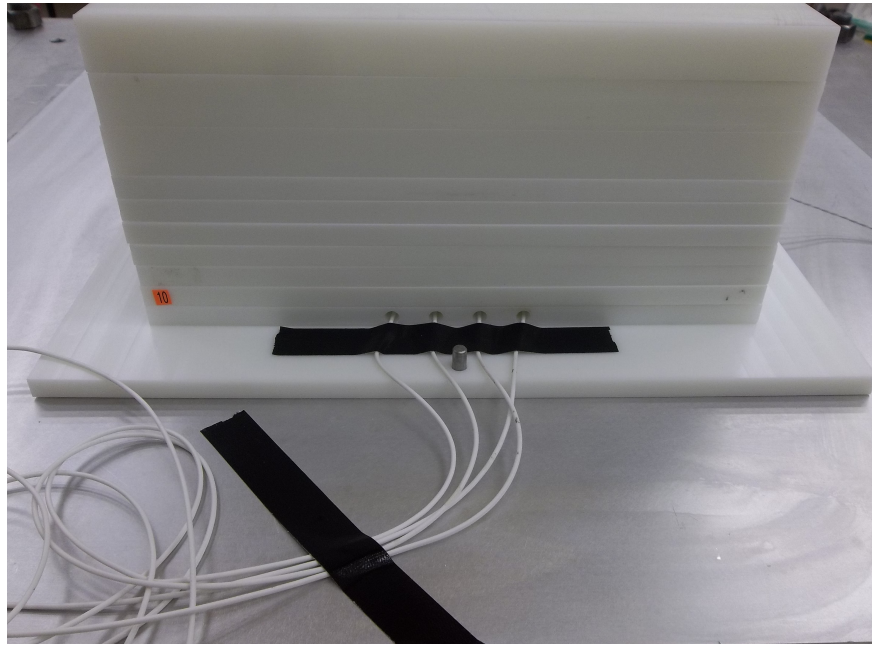


**Figure 4: Top Half of Class Foils on Planet Critical Assembly with the  $^3\text{He}$  Tubes in Place.**

shown in Fig. 5 using data from Table 1.

The second method was to measure fully assembled stacks where units were removed. Measurements were taken containing 15, 14, 13, 12, 11, 10, and 5 units. The gap between 10 and 5 was unintended, but rather a result of limited time with the material. During these various configuration changes, the stack was shifted several times to ensure the detection system never strayed more than 2 units from the center of the stack. Additionally, the  $k_{eff}$  of each of these cases was estimated using the mass comparison to the critical configuration [19].

$$k_{eff} = \left( \frac{m}{m_c} \right)^{0.25} \quad (10)$$

**Table 1:  $\alpha$  as a Function of Separation for the 16 Foil Configuration.**

Mils from Critical	Inverse CR (s/count)	$\alpha$ (1/s)
34	7.809E-6	-258.2
63	1.209E-5	-280.1
94	1.967E-5	-341.0

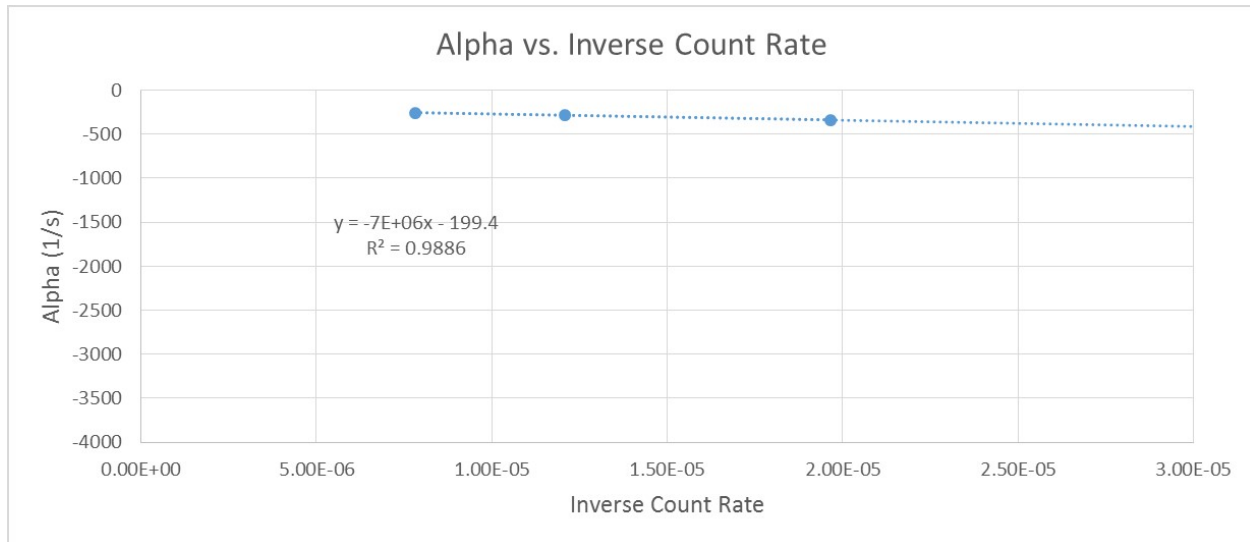


**Figure 5: Alpha versus Inverse Count Rate Plot used to Determine the Value of the  $\alpha$ -eigenvalue.**

### 3.2. Calculation Results

Two different types of calculations were completed for this experiment. The first were a series of k-code MCNP<sup>®</sup> \* calculations to determine the assumed reactivity in each case. The second set of calculations were executed in fixed source mode of MCNP to mimic the actual experiment. These calculations provide data much like that given in the experiment and are analyzed in an identical manner. For both sets of calculations, MCNP version 6.2 was used with the ENDF/B-VI cross-sections.

### 3.3. Combined Results

The best method available to calculate subcritical reactivity for this system is a comparison to k-code MCNP. This comparison turned out as expected, indicating that at some subcritical multiplication  $\alpha$  is no longer linearly related to the reactivity of the system. This result is shown using the data in Table 2 visualized by Fig. 6. In an ideal world, the slope of the comparison of reactivities shown in Fig. 6 would be 1. The slope differs due to small differences between the calculations and experiment. These deviations are caused by things such as gaps, nuclear data, etc.

\*MCNP<sup>®</sup> and Monte Carlo N-Particle<sup>®</sup> are registered trademarks owned by Los Alamos National Security, LLC, manager and operator of Los Alamos National Laboratory. Any third party use of such registered marks should be properly attributed to Los Alamos National Security, LLC, including the use of the designation as appropriate. For the purposes of visual clarity, the registered trademark symbol is assumed for all references to MCNP within the remainder of this paper.

**Table 2: Experimental and calculated data related to system reactivity as a function of the number of foils used.**

# of Foils	Calculated $k_{eff}$	$\rho_{CALC}(\$)$	$\alpha_{EXP} (s^{-1})$	$\rho_{EXP} (\$)$	Expected $k_{eff}$
15	0.993	-0.66	-340.4	-0.71	0.994
14	0.976	-2.90	-745.8	-2.74	0.977
13	0.954	-5.87	-1253.2	-5.28	0.959
12	0.931	-9.09	-1759.9	-7.82	0.940
11	0.905	-12.91	-2352.2	-10.80	0.920
10	0.876	-17.48	-3063.1	-14.36	0.898
9	0.842	-23.31	N/A	N/A	N/A
8	0.802	-30.65	N/A	N/A	N/A
7	0.757	-40.03	N/A	N/A	N/A
6	0.703	-52.59	N/A	N/A	N/A
5	0.642	-69.65	-6830.7	-33.26	0.755

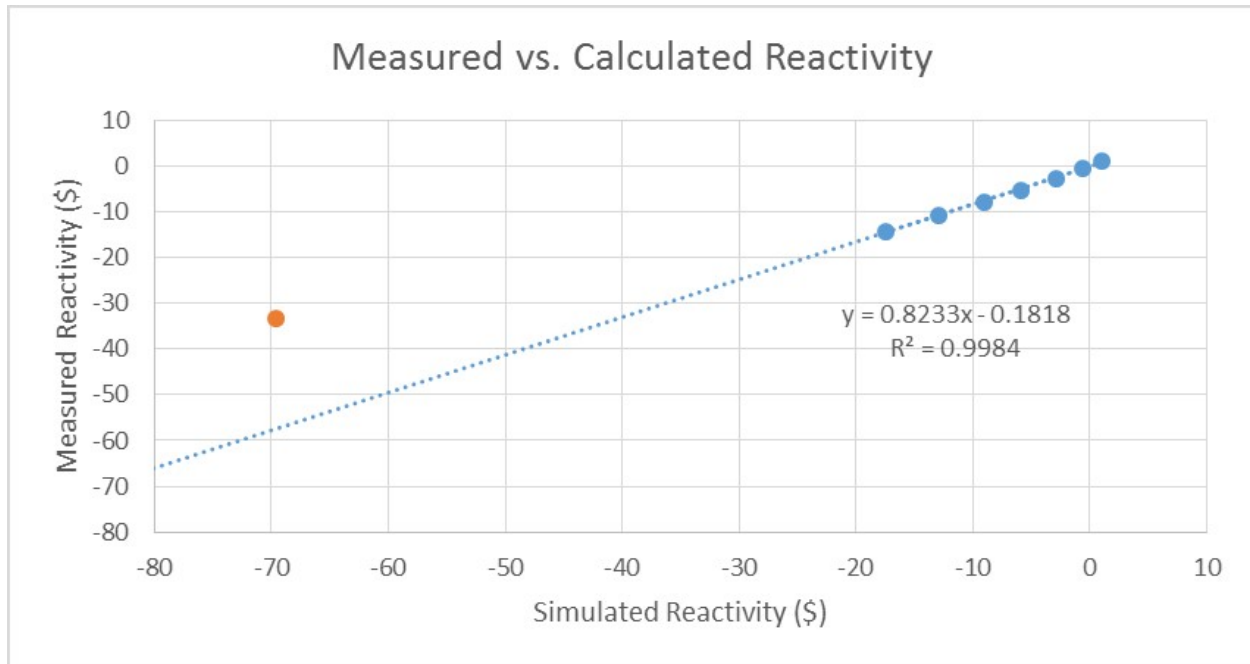


**Figure 6: Comparison of the Reactivity Calculated from the Measured  $\alpha$  to the Reactivity Calculated by MCNP.**

#### 4. CONCLUSIONS

Determination of subcritical reactivity using the Rossi- $\alpha$  method can be effectively performed for a thermal uranium system for values of  $0.87 < k_{eff} \leq 1.008$ . Measurements between  $k_{eff} = 0.87$  and  $k_{eff} = 0.64$  have not yet been completed. In the future, this range will likely be reduced, to narrow the range at which  $\alpha$  is no longer linearly related to the reactivity of the system. This work will likely translate similarly to fast uranium systems, but would require a data acquisition upgrade at NCERC so that the extremely fast decays can be measured. In the future, calculations and experiments will be performed on a fast system in an attempt to compare to this work.

#### ACKNOWLEDGEMENTS

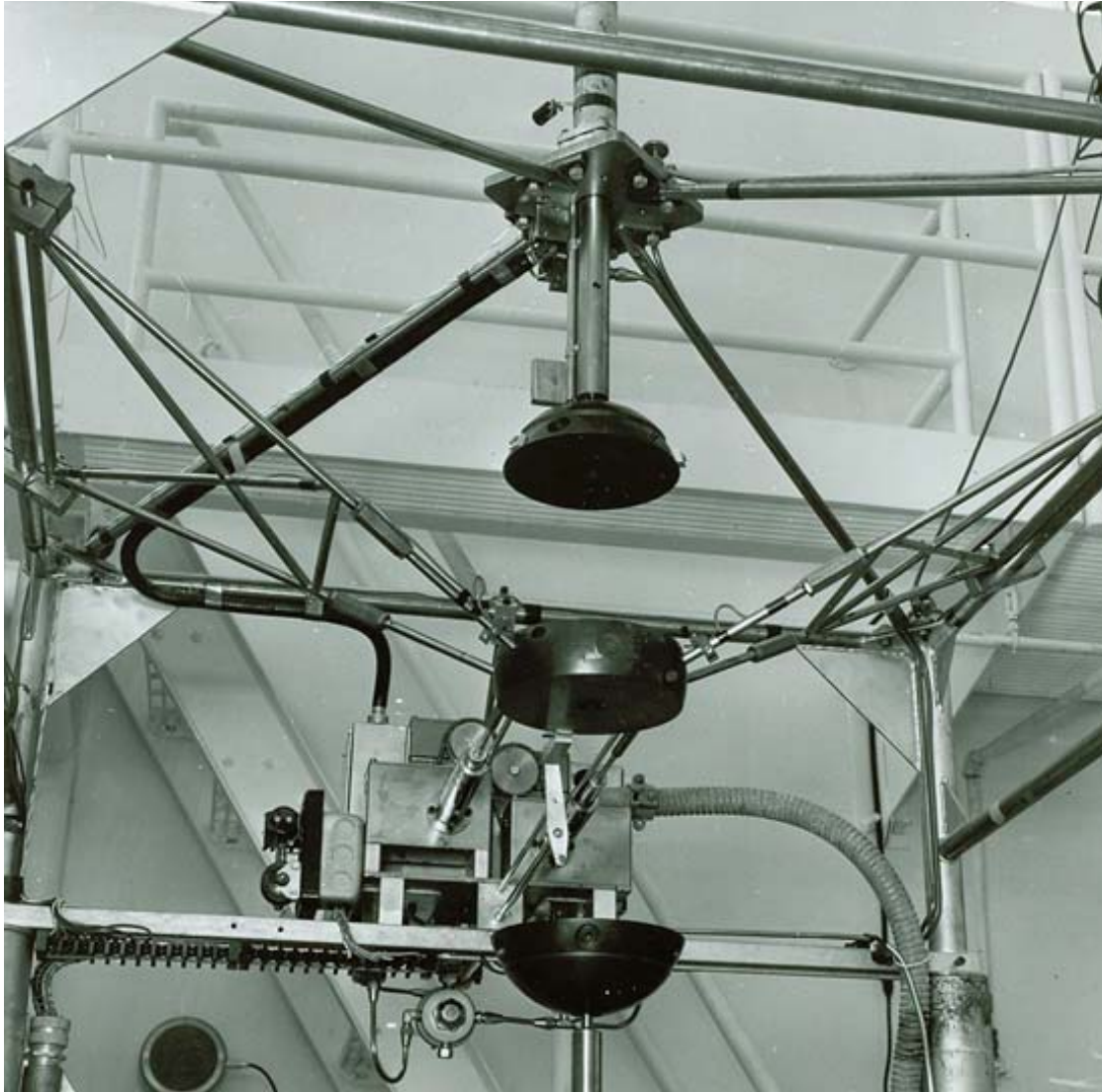
This work is supported in part by the DOE Nuclear Criticality Safety Program, funded and managed by the National Nuclear Security Administration for the Department of Energy.

#### REFERENCES

- [1] R. Feynman. "Statistical Behavior of Neutron Chains." Technical Report LA-591(DEL), Los Alamos National Laboratory, Los Alamos, NM (1946).
- [2] G. E. McKenzie. "Modern Rossi Alpha Measurements." *Masters Thesis* (2014).
- [3] J. Orndoff and C. Johnstone. "Time Scale Measurements by the Rossi Method." Technical Report LA-744, Los Alamos National Laboratory, Los Alamos, NM (1949).

- [4] K. L. Klain. “Determination of the Optimal Time Bin Width for the Rossi-Alpha Analysis of Highly Subcritical Fast Metal Systems.” *ANS Winter Proceedings* (2017).
- [5] H. C. Paxon and G. E. Hansen. “Critical Assemblies and Associated Measurements.” Unpublished.
- [6] G. R. Keepin. *Physics of Nuclear Kinetics*. Addison-Wesley, Reading, MA (1965).
- [7] R. E. Uhrig. *Random Noise Techniques in Nuclear Reactor Systems*. Ronald, New York, NY (1970).
- [8] M. M. R. Williams. *Random Processes in Nuclear Reactors*. Maxwell House, Elmsford, NY (1974).
- [9] G. E. Hansen. “The Rossi Alpha Method.” Technical Report LA-UR-85-4176, Los Alamos National Laboratory, Los Alamos, NM (1985).
- [10] G. Spriggs, G. Hansen, E. Martin, E. Plassman, R. Pederson, J. Schlessler, T. Krawczyk, G. Smolen, and J. Tanner. “Subcritical Measurements of the WINCO Slab Tank Experiment using the Source-jerk Technique.” *ANS Conference Proceedings* (1989).
- [11] F. de Hoffman. “Statistical Fluctuations in the Water Boiler and Time Dispersion of Neutrons Emitted per Fission.” Technical Report LA-101, Los Alamos National Laboratory, Los Alamos, NM (1944).
- [12] C. P. Baker. “Time Scale Measurements by the Rossi Method.” Technical Report LA-617, Los Alamos National Laboratory, Los Alamos, NM (1947).
- [13] M. Hayashi. “Comments on” Neutron Lifetime, Fission Time, and Generation Time.”” *Nuclear Science and Engineering*, **volume 121**, pp. 492–492 (1995).
- [14] F. de Hoffmann. “Criticality of the Water Boiler and Effective Number of Delayed Neutrons.” Technical Report LA-183, Los Alamos Scientific Lab. (1944).
- [15] R. P. Feynman, F. De Hoffmann, and R. Serber. “Dispersion of the neutron emission in U-235 fission.” *Journal of Nuclear Energy* (1954), **volume 3**(1-2), pp. 64IN9–69IN10 (1956).
- [16] T. Cutler, J. Bounds, T. Grove, J. Hutchinson, D. Hayes, and R. Sanchez. “A New Critical Experiment in Support of the Nuclear Criticality Safety Class.” *ICNC Conference Proceedings* (2015).
- [17] General Electric. *RS-P4-0203-201* (2010).
- [18] General Electric. *SS-P4-0203-201* (2010).
- [19] J. D. Hutchinson, T. E. Cutler, R. G. Sanchez, M. V. Mitchell, and D. K. Hayes. “Investigation of keff Versus Fraction of Critical Mass.” *ANS Conference Proceedings* (2014).

## **APPENDIX B**



 **Los Alamos**  
NATIONAL LABORATORY  
— EST. 1943 —

Delivering science and technology  
to protect our nation  
and promote world stability



Operated by Los Alamos National Security, LLC for the U.S. Department of Energy's NNSA

# Limits on Subcritical Reactivity Determination Using Rossi- $\alpha$ and Related Methods

Physor Conference- Cancun,Mx



**G. McKenzie IV**

April 2018

# Overview

- **Prompt Neutron Decay Constant**
- **Innovation**
- **Theory**
- **Experiment**
- **Calculation**
- **Analysis**
- **Results**
- **Conclusions**

# Prompt Neutron Decay Constants

- **Rate at which the prompt neutron population decays as a function of time.**
- **At DC comprises the fundamental  $\alpha$ -eigenvalue.**
- **Useful for neutron spectrum hardness comparisons in critical experiments.**
- **Useful for determining neutron lifetime of a system.**
- **Used to measure subcritical reactivity in a system.**

<b>Assembly</b>	<b><math>\alpha_{DC}</math> (1/s)</b>
Lady Godiva	$-1.1 \times 10^6$
Godiva IV	$-8.4 \times 10^5$
Topsy (Oy(94) w/ NU reflector)	$-3.7 \times 10^5$
Zeus	$-8.9 \times 10^4$
Zeus LEU Lead	$-5.6 \times 10^4$
Zeus HEU Lead	$-3.8 \times 10^4$
Sheba	-200

# Innovation

- **Prompt neutron decay constant measurements (Rossi-  $\alpha$ , pulsed neutron source, etc.) can be used to determine subcritical reactivity.**
- **Users of subcritical systems (example ADS) are interested in real time measurement of subcritical reactivity.**
- **These methods rely on the assumptions made during derivation of point reactor kinetics equations.**
  - Namely the separability of the spatial and time neutron fluxes.
  - Near critical time dependent flux is constant and separable.
- **The experimental determination of the threshold of non-linearity between  $\alpha$  and reactivity is the goal of this work.**
  - This measurement would be the first attempt to measure the linear to non-linear transition invalidating the assertion that subcritical reactivity can be inferred from  $\alpha$ :
    - $\rho = 1 - \alpha(\alpha_{DC}^{-1})$

# Theory – Types of Neutrons

## Prompt Neutrons

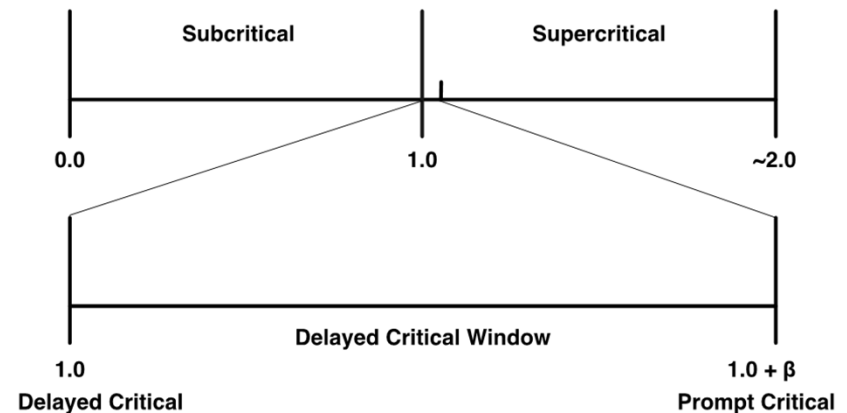
- **Emitted directly during fission process.**
  - $\sim 10^{-14}$  seconds after fission event
- **$\sim 2$  MeV of energy.**

## Delayed Neutrons

- **Emitted by daughter nuclei (fission fragments) as a nuclear decay from a metastable state.**
- **Occur milliseconds to seconds after fission.**
- **keV level of energy.**

## Theory – Effect of Delayed Neutrons on Criticality

- A chain reaction sustained only by prompt neutrons is called prompt critical.
- The prompt multiplication factor  $k_p$  is a measure of how the prompt fission rate grows or dissipates similarly to  $k_{\text{eff}}$  which considers all neutrons.
- A critical chain with all neutrons considered is called delayed critical.

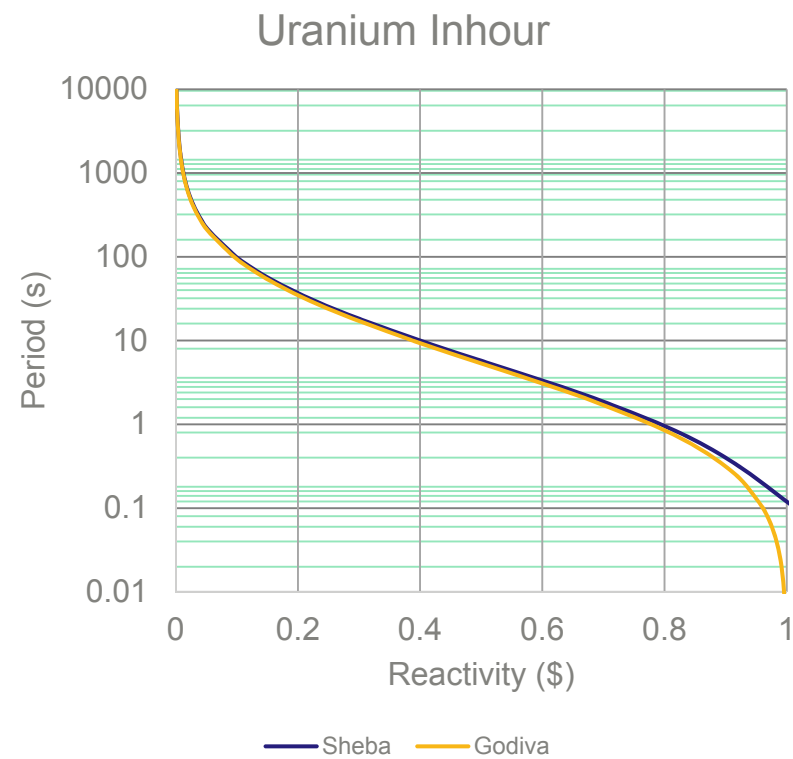


# Theory – Reactivity

- **Reactivity is a measure of how far a system is away from delayed critical.**

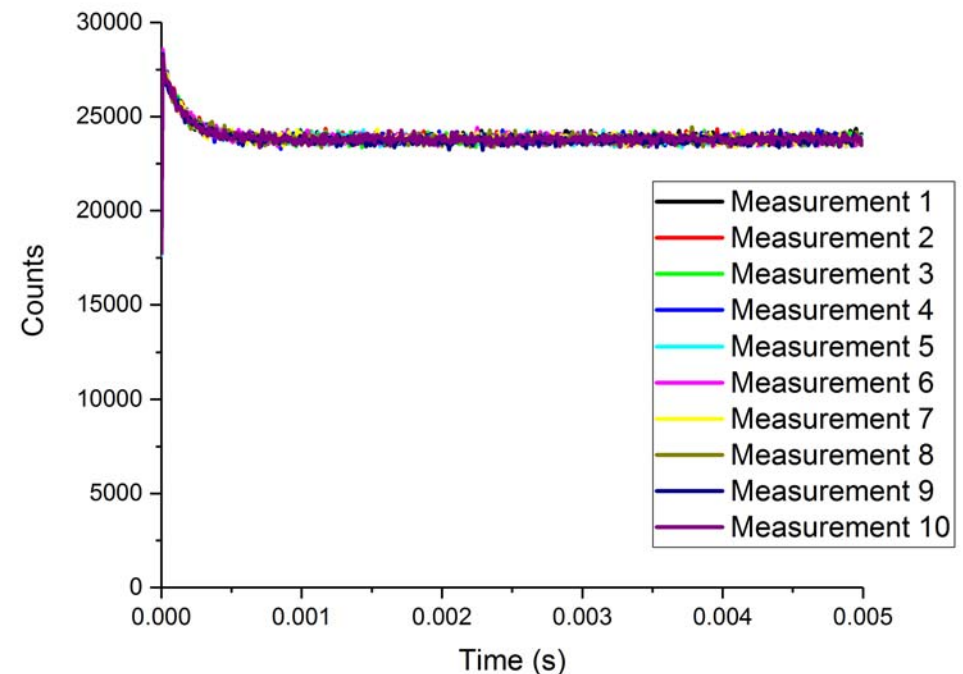
- $\rho_{\$} = \frac{k_{eff}-1}{k_{eff}\beta_{eff}}$

- Has units of dollars and cents
- Prompt critical = 1\$
- Delayed critical = 0\$



## Theory – Prompt Neutron Decay Constant

- The prompt neutron decay constant  $\alpha$  is the rate at which the prompt neutron population changes as a function of time.
- $$\alpha = \frac{k_p - 1}{l}$$
- Measureable quantity is  $\alpha$ , used to infer parameter of interest neutron lifetime,  $l$ .
- At delayed critical, this constant is the  $\alpha$ -eigenvalue of the system.
- $$\alpha_{DC} = \frac{-\beta}{l}$$
- At prompt critical  $\alpha = 0$ .



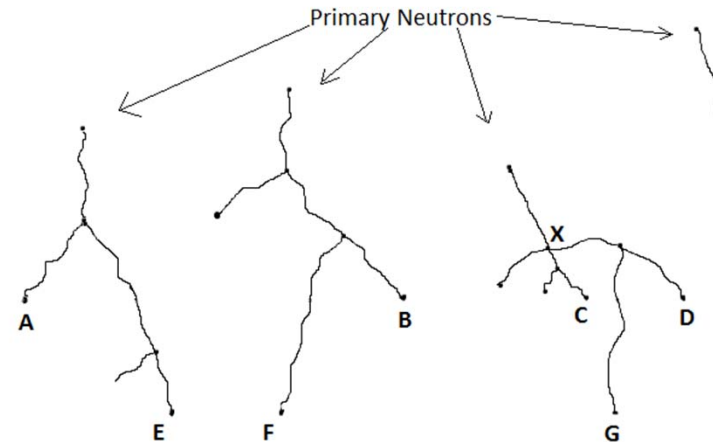
# Theory – Prompt Neutron Decay Constant cont.

## Correlated Neutrons

- Neutrons that have a common fission ancestor.
- Must all be prompt neutrons.

## Accidental Neutrons

- Neutrons that do not have a common fission ancestor.
- Include delayed neutrons, source neutrons, and prompt neutrons from different fission chains.



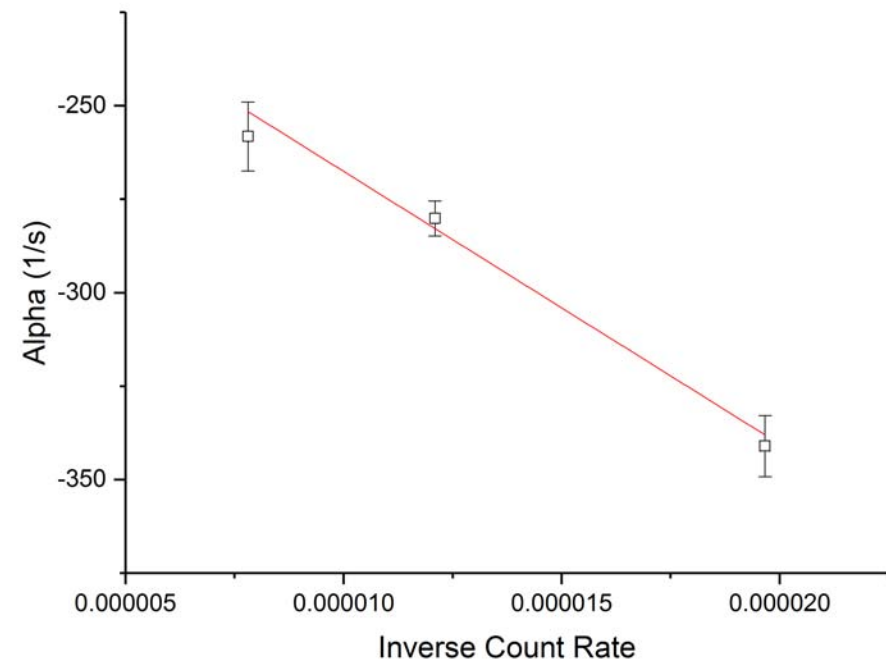
Every branching signifies a fission.

## Theory – Prompt Neutron Decay Constant cont.

- **The prompt neutron decay constant is calculated by measuring the correlations between neutrons emitted by a fissioning system.**
- **Rossi- $\alpha$  is an autocorrelation of neutron detection events.**
  - Combination of the probability of detecting a neutron from a fission chain and also detecting a second neutron from that same chain.
- $p(t) = A + Be^{at}$ 
  - A is related to the population of accidental neutrons.
    - Typically related to the source and multiplication of the system.
  - B is related to the population of correlated neutrons.
    - The probability of detecting correlated neutrons drops exponentially with time (if the system is below prompt critical), so the exponential term is included with the correlated term.

## Theory – Determine $\alpha$ -eigenvalue

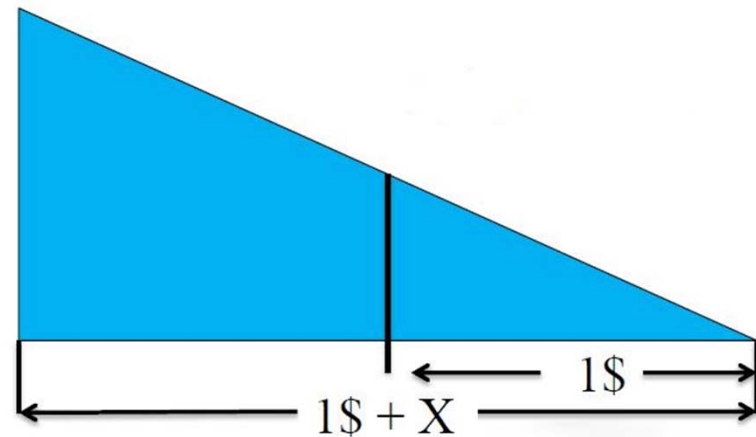
- **The  $\alpha$ -eigenvalue can be determined two ways.**
  - Direct measurement at delayed critical.
  - Inference using two or more subcritical data points.
    - Plot  $\alpha$  versus the inverse count rate.
    - The y-intercept is the  $\alpha$ -eigenvalue.
    - Example shown on the right.



## Theory – Determine Reactivity from $\alpha$

- Reactivity is calculated from  $\alpha$  using the  $\alpha$ -eigenvalue and the known value of reactivity and  $\alpha$  at prompt critical ( $\rho=1, \alpha=0$ ).

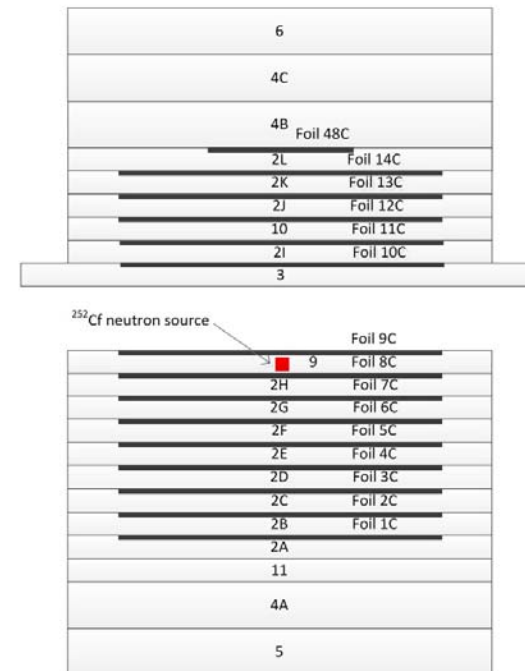
- $$\rho = \frac{\alpha_{DC} - \alpha}{\alpha_{DC}}$$



## Experiment – Critical Assemblies cont.

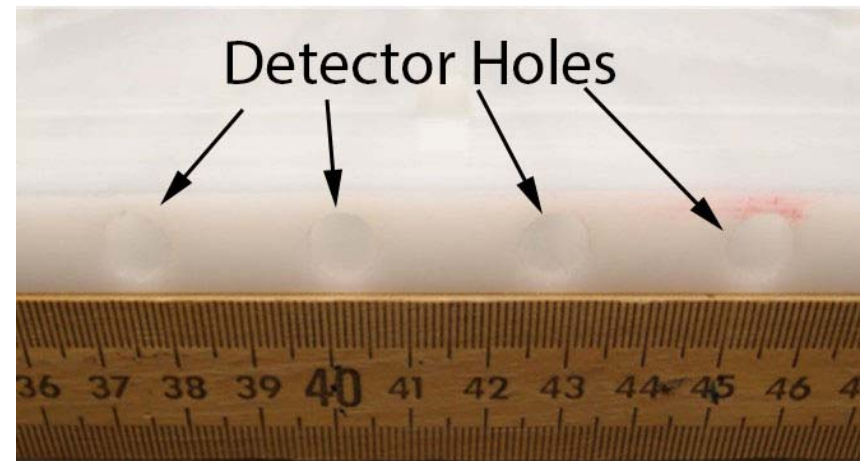
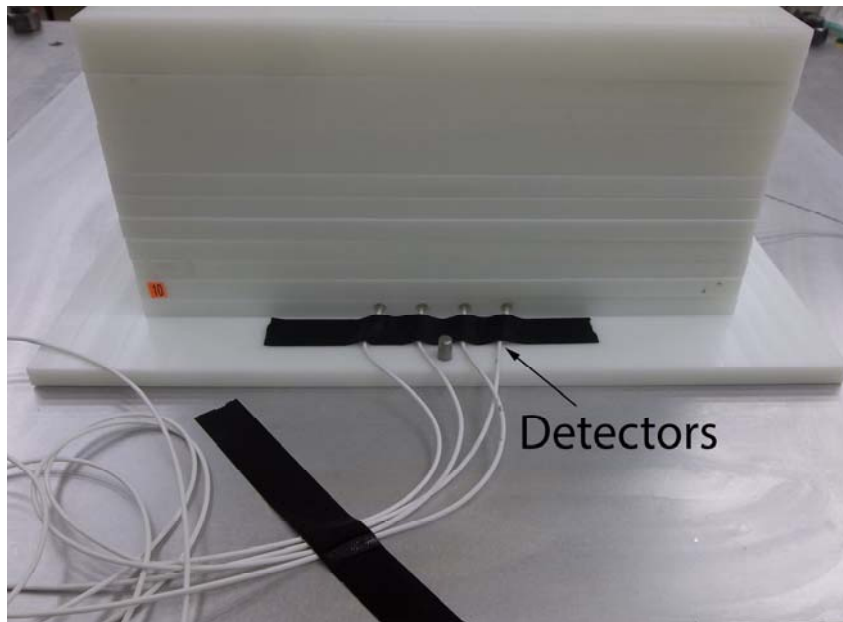
### Polyethylene Class Foils

- Thermal metal critical assembly.
- Designed to mimic solution with minimum critical mass.
- Fuel consists of 3 mil thick foils of 93% enriched  $^{235}\text{U}$  weighing approximately 69 grams each.
- ~1 kg of material in clean critical configuration.
- On Planet critical assembly:
  - Reactivity controlled through separation of two subcritical masses.





## Experiment – Critical Assemblies cont.



## Experiment – Critical Assemblies cont.

Reactivity determined from the O'Dell relation

- Once a critical configuration was established. The  $k_{eff}$  of each expected configuration can be estimated using the O'Dell relation.
  - $k_{eff} \approx \left(\frac{m}{m_c}\right)^{0.25}$
- Used to estimate reactivity prior to experiment execution.

# of Units	$k_{eff}$	$\rho$ (\$)	$\alpha$ (1/s)
15	0.995	-0.59	-317.4
14	0.978	-2.65	-727.6
13	0.96	-4.9	-1176.2
12	0.941	-7.38	-1670.1
11	0.921	-10.12	-2218.3
10	0.899	-13.21	-2832.7
9	0.876	-16.7	-3529.1
8	0.85	-20.71	-4329.6
7	0.822	-25.41	-5266.1
6	0.791	-31.03	-6386.9
5	0.756	-37.96	-7769.5

# Experiment – Critical Assemblies cont.

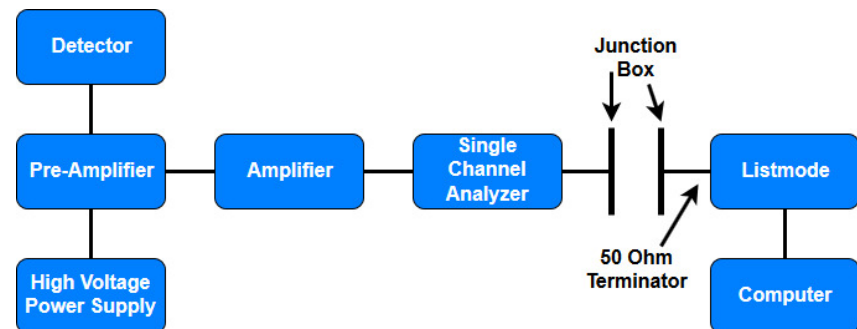
## Critical Configuration – 16 Foils



6 Poly		1"
4B Poly		1"
4C Poly		1"
2N Poly	10C HEU	0.5"
2M Poly	11C HEU	0.5"
2H Poly	12C HEU	0.5"
2G Poly	13C HEU	0.5"
2E Poly	14C HEU	0.5"
10 RTD	15C HEU	0.5"
Rossi Alpha Plate	16C HEU	0.5"
3 Membrane Poly	17C HEU	0.5"
2C Poly	18C HEU	0.5"
2I Poly	19C HEU	0.5"
2J Poly	20C HEU	0.5"
2K Poly	21C HEU	0.5"
2L Poly	22C HEU	0.5"
2F Poly	23C HEU	0.5"
2D Poly	24C HEU	0.5"
9 Poly Source	25C HEU	0.5"
11 Poly		0.5"
4A Poly		1"
5 Poly		1"

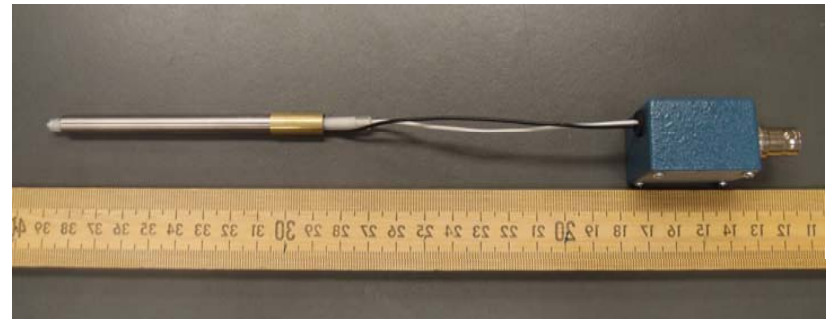
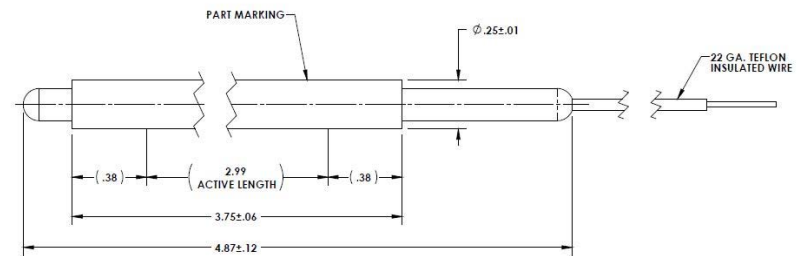
# Experiment – Neutron Detection System

- Consists of largely commercial off the shelf equipment.
- List-mode module is custom LANL designed and built module.
  - Time tags detection events.



## Experiment – Neutron Detection System cont.

- **Detector is Reuter-Stokes 40 atm 0.25" diameter, 4" long  $^3\text{He}$  detector.**
  - Other detectors could be used.
  - Chosen because of its fast recovery and size.



## Experiment – Execution

### Godiva IV

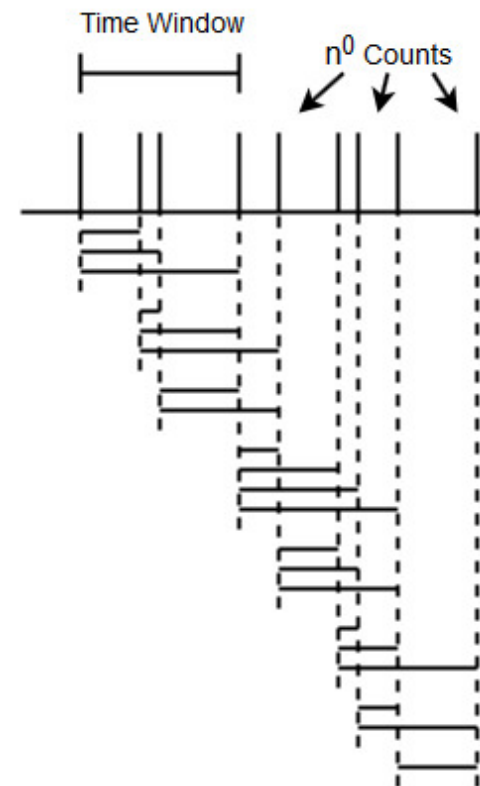
- **Three measurements were attempted using the pulsed source technique.**
  - Pulsed source was used in an attempt to maximize signal to noise ratio.
  - Three measurements taken at 50, 100, and 150 cents subcritical.
- **Measurements did not provide sufficient statistics to determine the  $\alpha$ -eigenvalue.**
- **Measurements would require a new detection system and proof testing of the new system.**

### Polyethylene Class Foils

- **Three measurements completed using separation of the critical configuration (34, 63, and 94 mils).**
  - Used to determine the  $\alpha$ -eigenvalue.
- **7 other measurements on fully closed configurations where foils were removed to decrease reactivity (15, 14, 13, 12, 11, 10, and 5 foils).**
  - Used to vary reactivity over large range.
  - $^{252}\text{Cf}$  source used

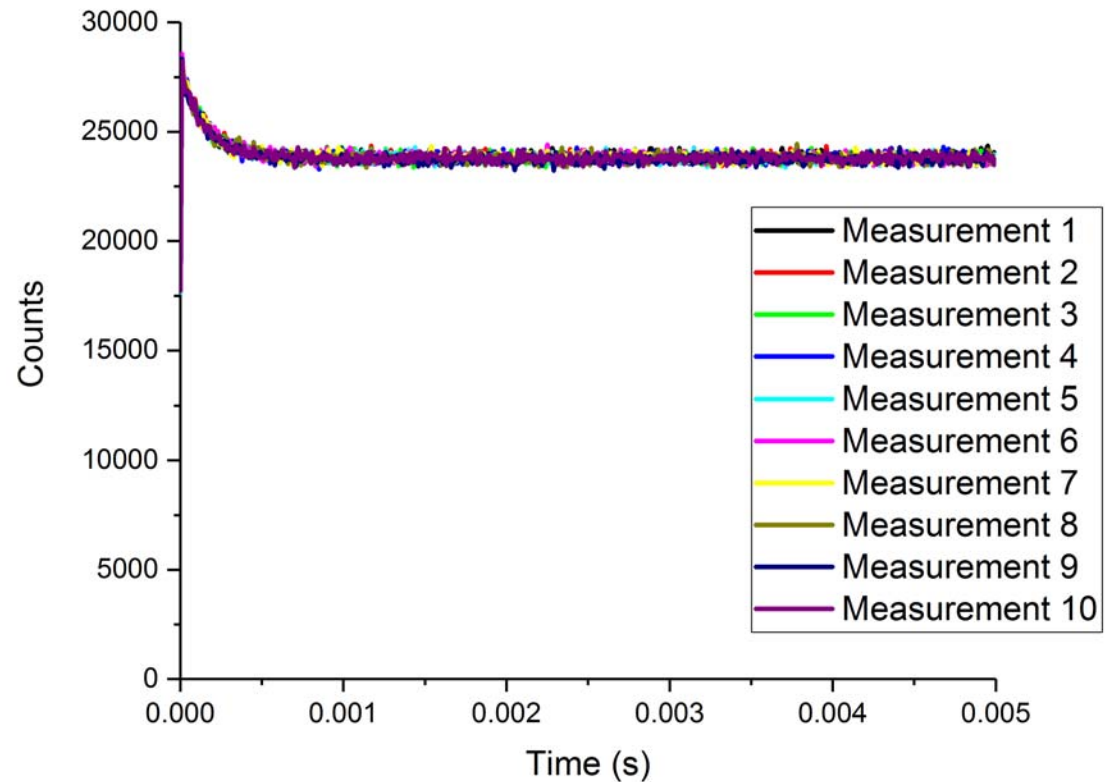
## Analysis – The Method

- **List-mode data is processed to be manipulated by specifically designed programs which determine  $\alpha$ .**
- **Data is reduced from initial form.**
- **Bins list-mode data based on time differences between detection events.**
- **This binning produces a decay histogram (if the system is sub-prompt critical).**
- **This histogram is fit using a non-linear exponential fit.**



## Analysis – The Code

- **Initial parameters for the code are set using previous experience.**
- **Example to the right shows a prompt neutron decay curve for the 5 foil case.**



# Analysis – Uncertainty

## Systematic Uncertainty

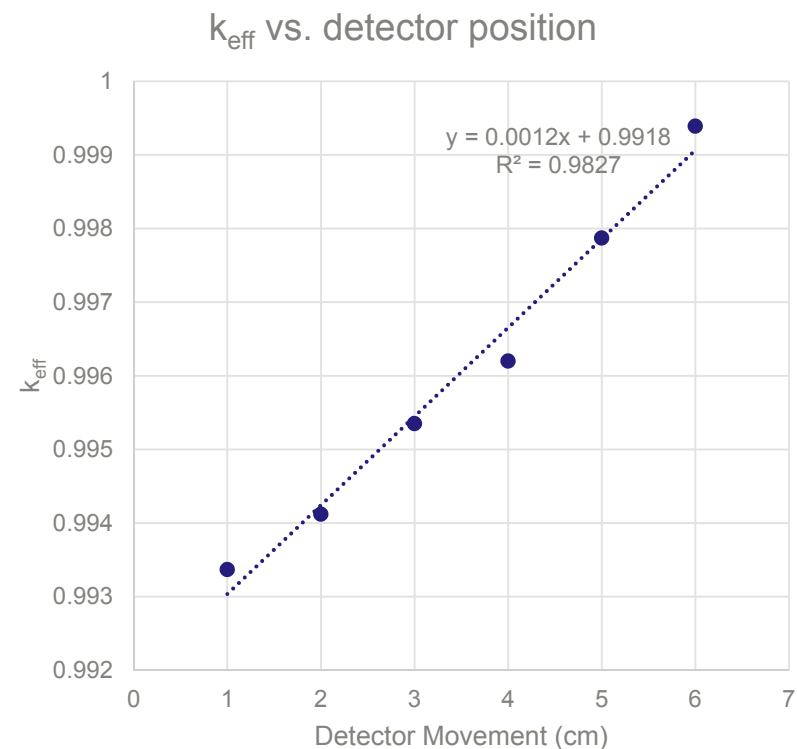
- **Uncertainty not due to chance, but rather introduced into the measurement.**
- **Uncertainty due to unknowns in fabrication or construction.**
- **Things like gaps between materials, dimensions, and masses of pieces of the experiment.**
- **These type of uncertainties may be similar between different configurations.**

## Statistical Uncertainty

- **Uncertainty due to natural fluctuations.**
- **If a measurement could be performed infinite times the average value should match the true mean.**
- **Statistical uncertainty quantifies how much the value obtained from a single measurement could deviate from the true mean.**

# Analysis – Systematic Uncertainty

- **Determined by perturbing MCNP simulation by known amounts to determine the sensitivity of a system to the perturbed parameter.**
- **This sensitivity can then be converted into an uncertainty.**
  - $U = S_x \Delta x$
  - $S = \frac{\Delta k}{\delta x}$
  - U – uncertainty
  - $S_x$ - sensitivity
  - $\delta x$  - perturbation of parameter
  - $\Delta x$  – expected variation in x



## Analysis – Systematic Uncertainty cont.

- **For this experiment, many of the parameters of interest for the systematic uncertainty come from HEU-MET-THERM-001.**
  - Same nuclear material
  - Slightly larger polyethylene plates.
  - Proven similar sensitivity by examining parameter with largest sensitivity.

### **Sources of uncertainty addressed.**

- Position of detectors in the plate.
- HEU mass
- Polyethylene plate mass
- Polyethylene plate dimensions
- Axial air gap
- **These sources of uncertainty listed are chosen with expert knowledge and experience.**
- **This list is not intended to be comprehensive but rather choose the most sensitive parameters.**

## Analysis – Systematic Uncertainty cont.

- Although almost certainly not independent each of these uncertainty values was considered independent and quadratically combined as a total uncertainty.
- This will overestimate, but bound the uncertainty attached to the measurement.
- Example of quadratic combination on the right.

$$\alpha = \frac{k_p - k_{eff}}{l}$$

$$\delta\alpha = \sqrt{\left(\frac{\partial\alpha}{\partial k_p} \delta k_p\right)^2 + \left(\frac{\partial\alpha}{\partial k_{eff}} \delta k_{eff}\right)^2 + \left(\frac{\partial\alpha}{\partial l} \delta l\right)^2}$$

## Results – Polyethylene Class Foils cont.

Source of Uncertainty	Parameter Variation in Calculation	Calculated Effect of Variation	Standard Uncertainty of Parameter	Standard Uncertainty in $\Delta k_{\text{eff}}$
Detector Position	0.393 in	$\pm 0.0012$	0.393 in	$\pm 0.0012$
HEU Mass	0.5291 g/cm <sup>3</sup>	$\pm 0.0055$	0.5291 g/cm <sup>3</sup>	$\pm 0.0055$
Poly Plate Mass	0.00125 g/cm <sup>3</sup>	$\pm 0.0014$	0.00042 g/cm <sup>3</sup>	$\pm 0.0004$
Poly Plate Dim.	0.1 in	$\pm 0.0015$	0.01/ $\sqrt{3}$ in	$\pm 0.00009$
Axial Air Gap	0.002 in	$\pm 0.0036$	0.002/ $\sqrt{3}$ in	$\pm 0.0021$
Total Uncertainty	Combined Total: $\pm 0.0060$			

## Results – Polyethylene Class Foils cont.

- Measurements were successfully completed on the Polyethylene Class Foils for 7 different configurations.
- 10 measurements were completed on each configuration.
- Statistical deviation between these measurements had a standard deviation of ~2%.
- Systematic uncertainty, mostly due to uncertainty on the fuel drive the uncertainty shown for each measurement in the chart to the right.

Units	$\alpha$ (s <sup>-1</sup> )	$\sigma_\alpha$ (s <sup>-1</sup> )	$\rho$ (\$)	$\sigma_\rho$ (\$)
15	-340.4	141.4	-0.71	0.71
14	-745.8	141.4	-2.74	0.72
13	-1253.2	141.7	-5.28	0.72
12	-1759.9	143.0	-7.83	0.74
11	-2352.2	142.1	-10.80	0.76
10	-3063.1	145.7	-14.36	0.81
5	-6830.7	199.3	-33.26	1.25

## Calculation - Methods

- **Baseline simulations were completed on each experimentally measured configuration.**
- **These simulations are designed to be linear to the reactivity determined from  $\alpha$ .**
- **All simulations completed using MCNP *KCODE*, which is subsequently converted to reactivity.**
- **A modified reactivity formula is used to determine the reactivity differences between the simulation and the critical experimental configuration.**
- $$\rho = \frac{k_{eff} - k_{eff}(DC)}{k_{eff} k_{eff}(DC) \beta_{eff}}$$
- **This equation determines the change in reactivity between the MCNP deck configured like the experiment and the experiment.**

## Results – Polyethylene Class Foils

- Simulations were used as the baseline reactivity to be compared to other simulations and the experimental data.
- *KCODE* MCNP simulations were run to determine  $k_{\text{eff}}$ .
- This  $k_{\text{eff}}$  is then converted to reactivity using  $\beta_{\text{eff}} = 0.0085$ .

Units	$k_{\text{eff}}$	$\sigma_k$	$\rho$ (\$)	$\sigma_\rho$ (\$)
15	0.993	2.6E-4	-0.54	0.03
14	0.976	2.8E-4	-2.66	0.03
13	0.954	2.7E-4	-5.45	0.03
12	0.931	2.5E-4	-8.49	0.03
11	0.905	2.7E-4	-12.08	0.04
10	0.876	2.6E-4	-16.38	0.04
9	0.842	2.6E-4	-21.87	0.04
8	0.802	2.6E-4	-28.78	0.05
7	0.757	2.7E-4	-37.60	0.06
6	0.703	2.4E-4	-49.43	0.06
5	0.642	2.4E-4	-65.48	0.07

## Calculation - Methods

Two calculational methods are used for comparison during this work.

### Definition of $\alpha$ method.

- Calculates values from the derived definition of  $\alpha$ .
- Takes as long as a converging *KCODE* MCNP<sup>®</sup> simulation.
- Performed as preliminary study of the value of  $\alpha$ .

- $$\alpha = \frac{k_p - 1}{l}$$

- Modified Version suggested by MCNP developers:

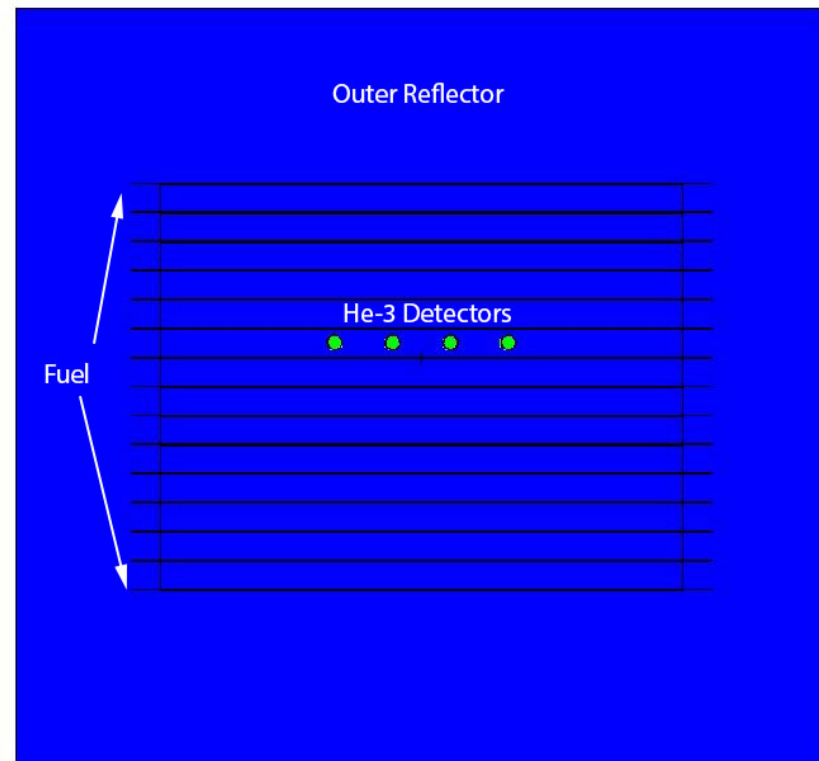
- $$\alpha = \frac{k_p - k_{eff}(DC)}{l}$$

### Simulated experiment method.

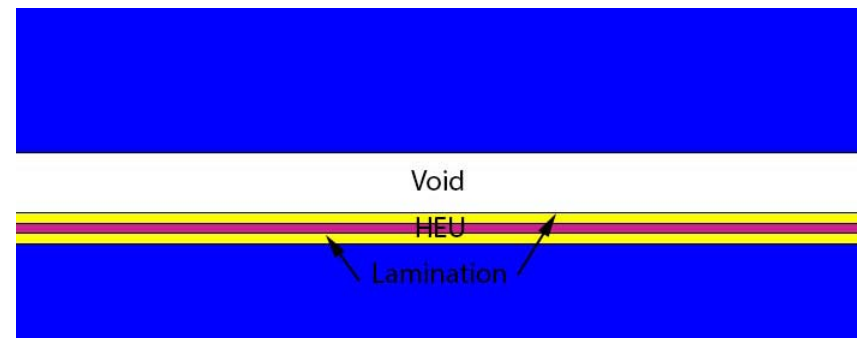
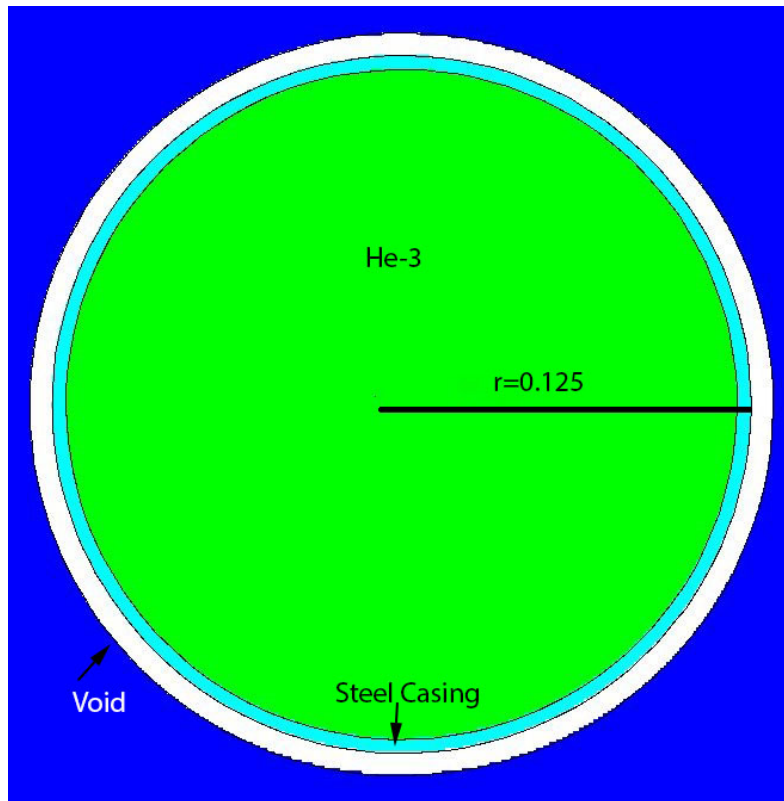
- Uses particle tracking to store the absorption events in He<sup>3</sup> and create output identical to experimental listmode data.
- Data is analyzed identically to the experimental data.
- Must be run in source mode with no variance reduction.
- Performed after the experiment for comparison.
- $$p(t) = A + Be^{\alpha t}$$

## Calculation – Polyethylene Class Foils

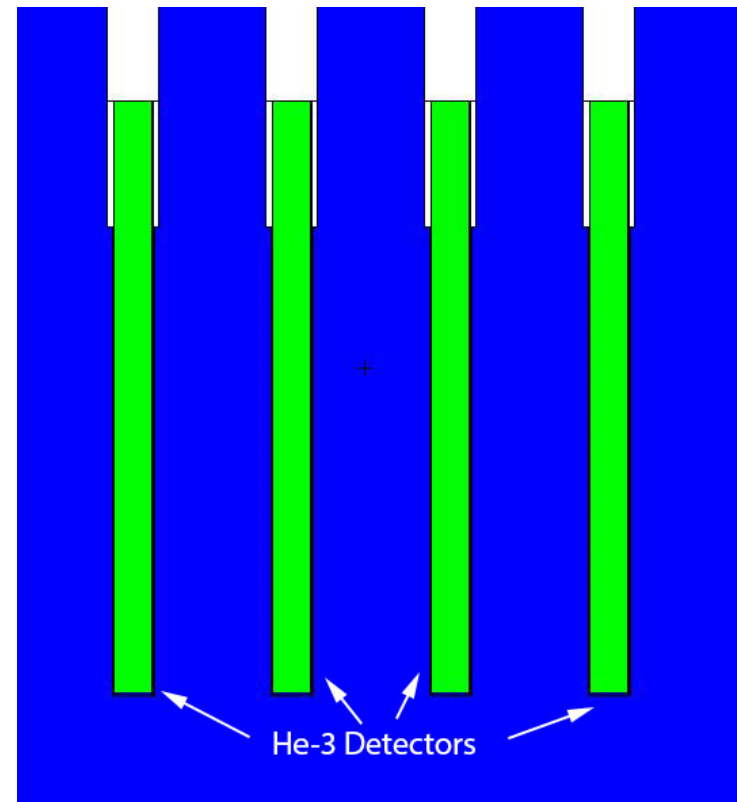
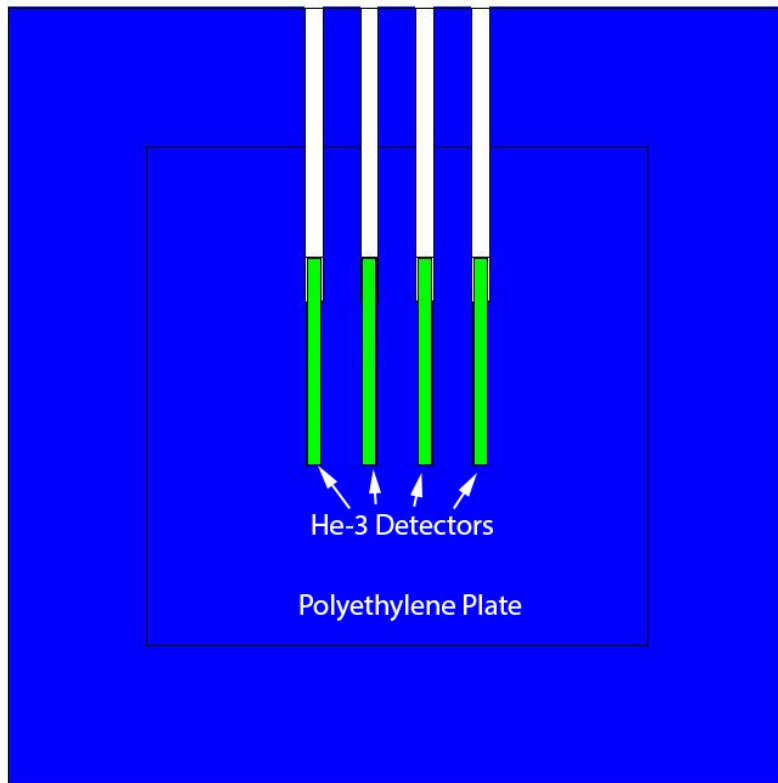
- **MCNP deck from the design process was used for simulations.**
- **Configurations with 15-5 foils were considered. Including the cases not experimentally measured.**
- **Simulations using both simulation methods described were performed on all cases.**



# Calculation – Polyethylene Class Foils cont.



# Calculation – Polyethylene Class Foils cont.



## Results – Polyethylene Class Foils cont.

Definition of  $\alpha$  method simulation results.

Units	$k_p$	$\sigma_k$	$\alpha$ ( $s^{-1}$ )	$\sigma_\alpha$ ( $s^{-1}$ )	$\rho$ (\$)	$\sigma_\rho$ (\$)
15	0.985	2.7E-4	-307.2	141.6	-0.54	0.71
14	0.968	2.6E-4	-704.4	141.6	-2.53	0.72
13	0.945	2.6E-4	-1235.2	141.6	-5.19	0.72
12	0.923	2.6E-4	-1758.6	141.6	-7.82	0.74
11	0.897	2.6E-4	-2360.5	141.6	-10.84	0.76
10	0.868	2.6E-4	-3041.6	141.6	-14.25	0.79
9	0.834	2.7E-4	-3842.2	141.6	-18.27	0.83
8	0.795	2.5E-4	-4761.8	141.5	-22.88	0.89
7	0.750	2.5E-4	-5802.4	141.5	-28.10	0.96
6	0.697	2.5E-4	-7067.6	141.5	-34.44	1.06
5	0.634	2.4E-4	-8528.6	141.5	-41.77	1.18

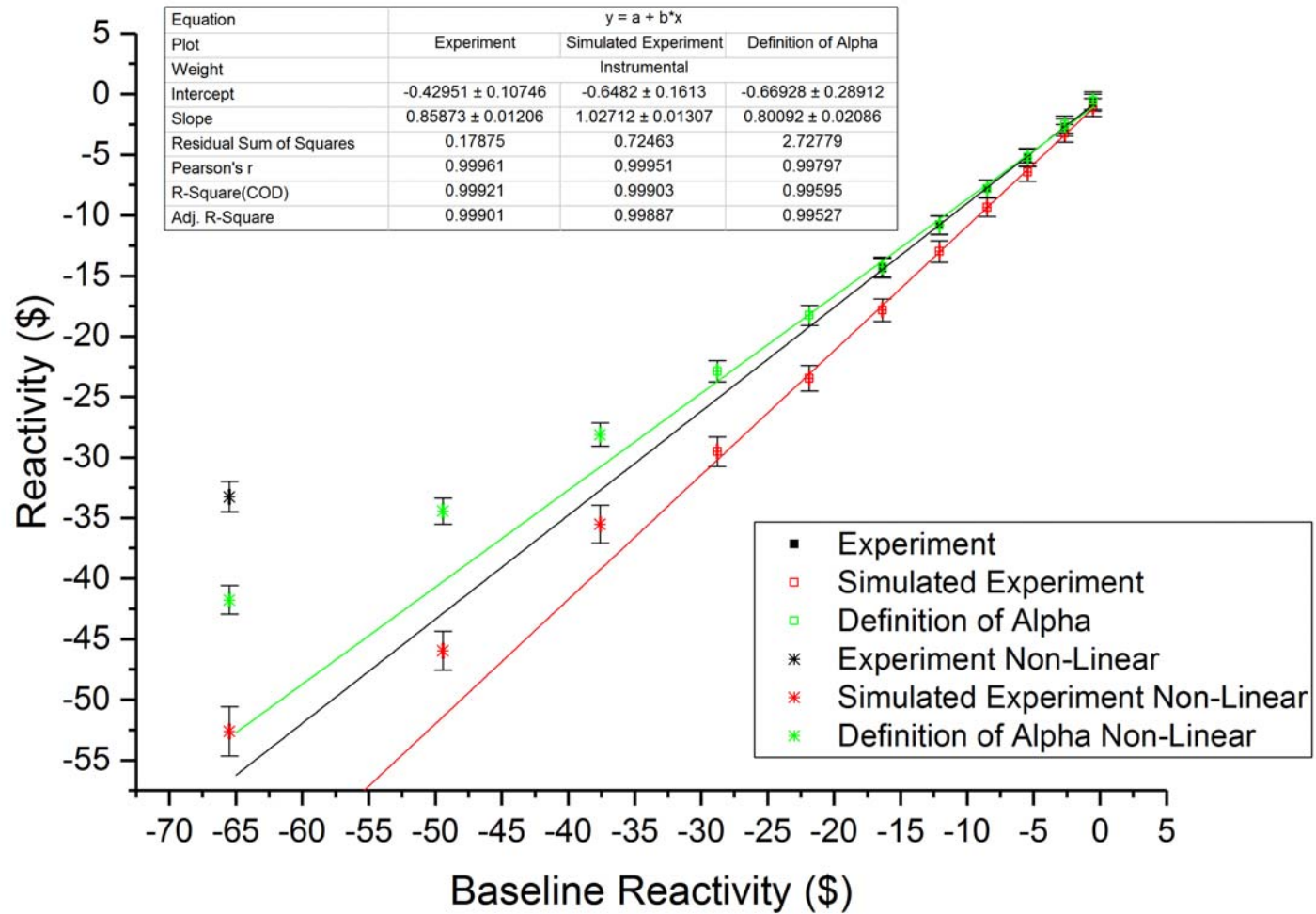
Simulated experiment simulation results

Units	$\alpha$ ( $s^{-1}$ )	$\sigma_\alpha$ ( $s^{-1}$ )	$\rho$ (\$)	$\sigma_\rho$ (\$)
15	-417.8	150.2	-1.10	0.76
14	-842.2	145.4	-3.22	0.74
13	-1483.9	148.4	-6.44	0.76
12	-2060.7	150.0	-9.33	0.79
11	-2791.1	163.3	-13.00	0.88
10	-3753.3	164.7	-17.82	0.93
9	-4878.1	180.5	-23.46	1.05
8	-6084.0	202.8	-29.51	1.22
7	-7283.5	266.9	-35.53	1.56
6	-9362.7	244.4	-45.95	1.61
5	-10689.6	331.4	-52.61	2.04

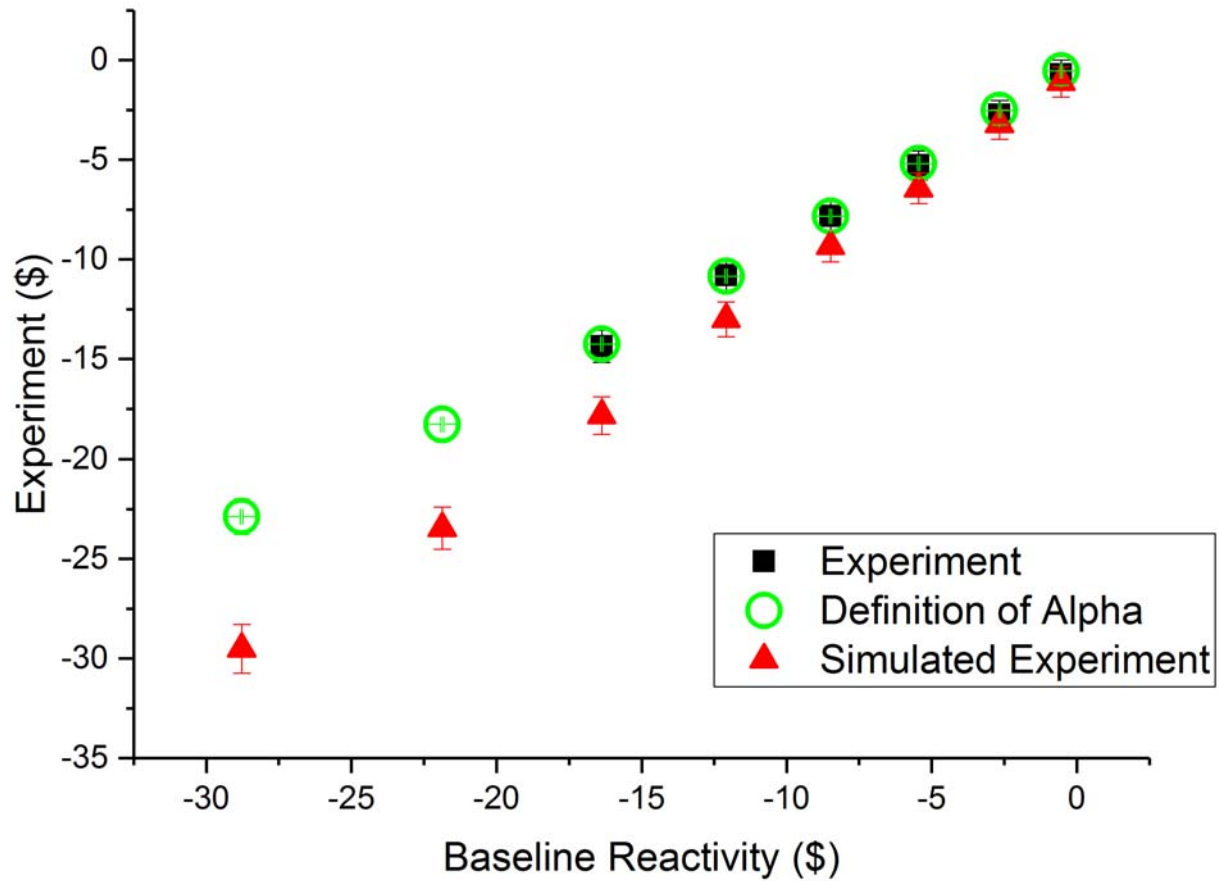
## Results – Polyethylene Class Foils cont.

- The results from the experiment and both simulations can then be plotted against the baseline reactivity determined through *KCODE* MCNP simulation.
- Additionally, a plot of the C/E for both experimental methods was created to examine each method.
- The likeness to experiment method has a fairly constant bias of ~20% higher.
- The definition of  $\alpha$  method has issues near critical.
  - Likely because the value of  $\alpha$  is approaching 0 and small deviations are more sensitive.
- The C/E for the 5 foil case is not shown in the graph because it was much larger for both methods.
  - ~1.6 for likeness to experiment, ~1.2 for the definition of  $\alpha$ .

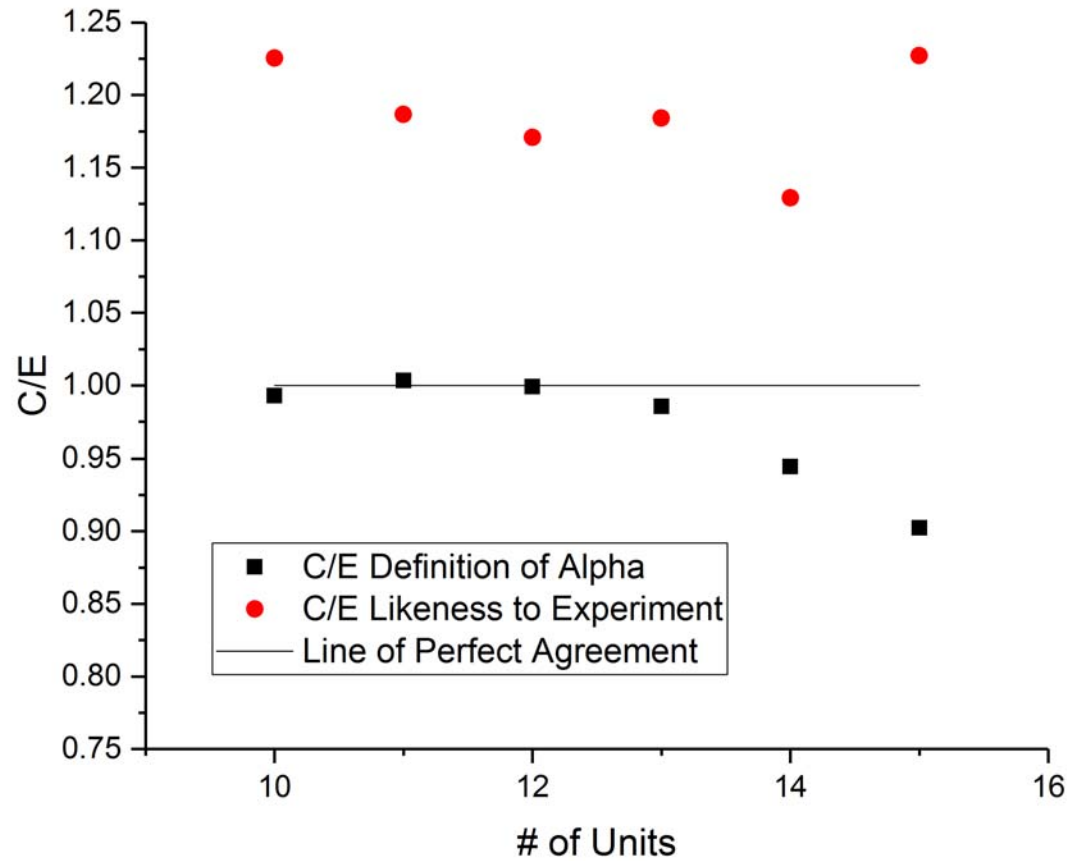
# Results – Polyethylene Class Foils cont.



## Results – Polyethylene Class Foils cont.



## Results – Polyethylene Class Foils cont.

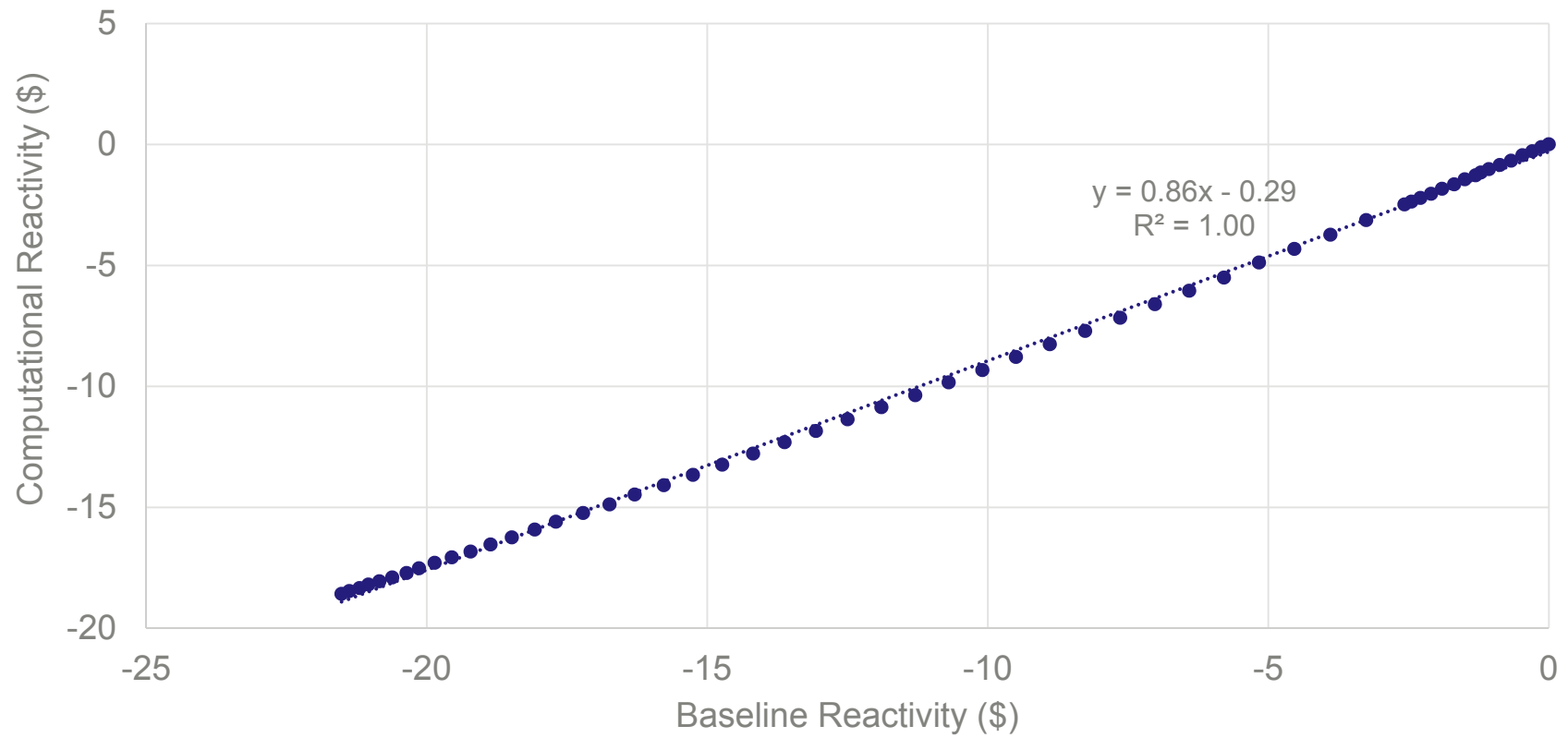


## Results – Godiva IV cont.

- If the results obtained from the Polyethylene Class Foils were to directly relate to the threshold of non-linearity for a fast metal system like Godiva IV, no non-linear region would be seen by measuring the Godiva IV system as its minimum reactivity is less than 25\$.
- This is confirmed through the preliminary definition of  $\alpha$  method simulations performed as shown by the graph on the following page.

# Results – Godiva IV cont.

Computational vs. Baseline Reactivity Godiva IV



## Conclusions

- **Successful in determining threshold of non-linearity using measurements of the prompt neutron decay constant on the Polyethylene Class Foils Assembly.**
  - First measurement of this transition.
  - Useful for NCERC operations and in the larger market of ADS systems.
- **The measurement threshold is experimentally determined to be between  $-65\% < \rho \leq -16\%$ .**
- **Because simulations agreed so well with the experiment, computations are used to narrow the threshold to occur between  $-38\% < \rho \leq -29\%$ .**
- **This result is important because it provides a method to determine subcritical reactivity without a measurement at delayed critical, and without careful restriction of other parameters.**
- **For more subcritical systems, other methods such as Feynman's Variance-to-Mean method should be applied to determine the system's state.**

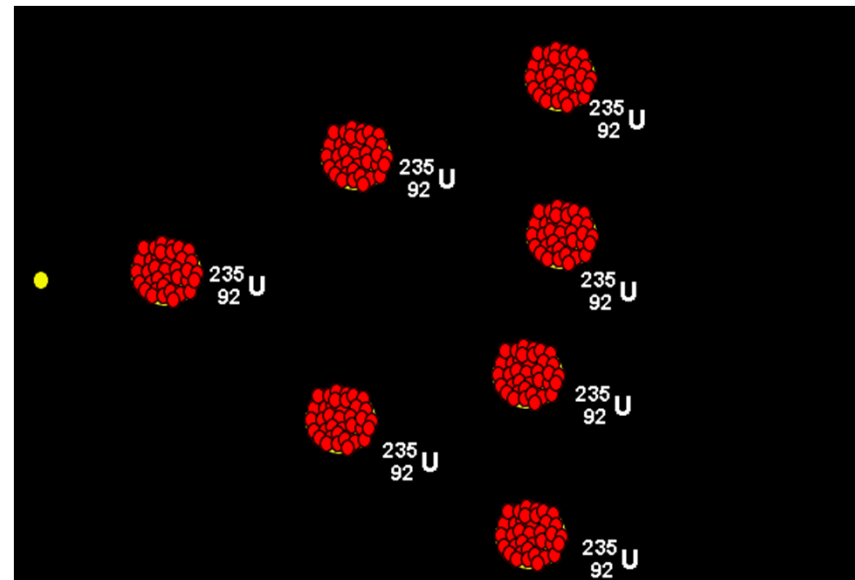
Special thanks to the critical experiments team at LANL and our operations team in Nevada. Many of the members have worked hard along side myself to make these measurements a possibility.

This work was supported in part by the DOE Nuclear Criticality Safety Program, funded and managed by the National Nuclear Security Administration for the Department of Energy.

Questions?

# Theory - Fission

- Fission is the splitting of an atom to create several daughter nuclei, neutrons, and other particles.
- Fission chains occur when neutrons released by one fission create another fission.
- Effective multiplication factor  $k_{\text{eff}}$  describes whether the fission rate in a system is growing or dissipating.



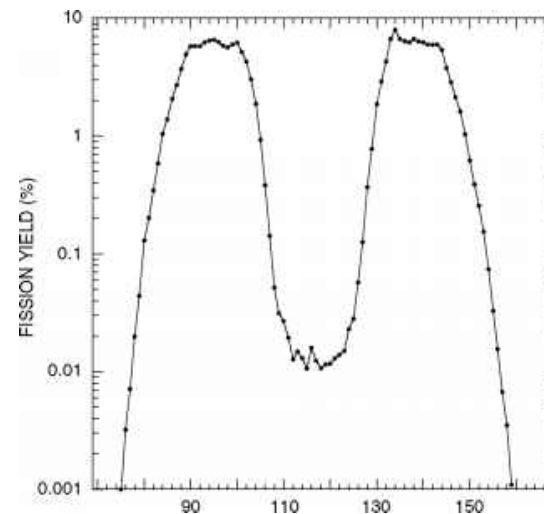
# Theory – Fission

- A critical system has a constant fission rate.
  - Each  $n^0$  in generation  $i$  is replaced by one  $n^0$  in generation  $i+1$ .

$$k_{eff} \begin{cases} < 1 & \textit{subcritical} \\ = 1 & \textit{critical} \\ > 1 & \textit{supercritical} \end{cases}$$

- A typical fission reaction is:

- $^{235}\text{U} + n^0 \rightarrow ^{236}\text{U}^* \rightarrow ff + n^0s + op$ 
  - ff = fission fragments
  - op = other particles
  - Total energy on the RHS is  $\sim 200\text{MeV}$



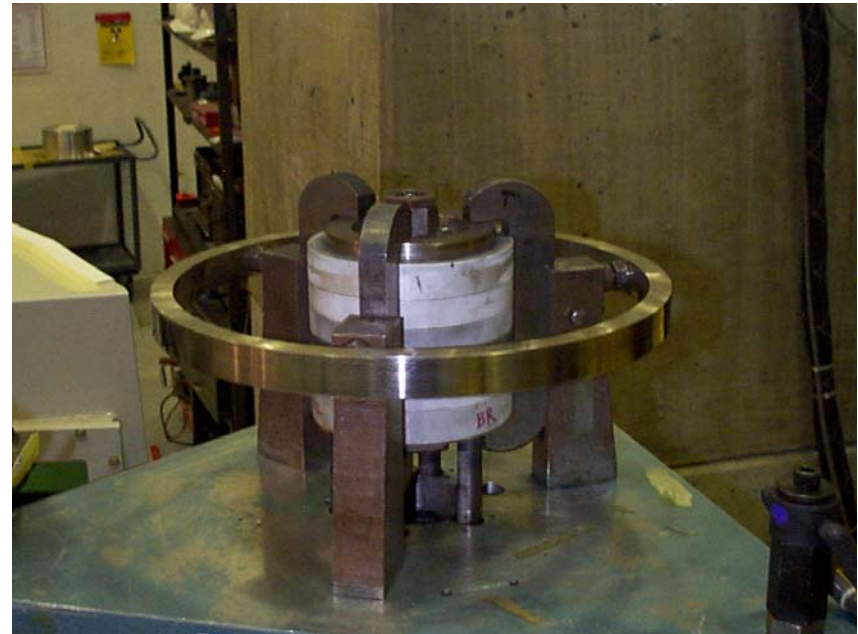
## Theory – Effect of Delayed Neutrons on Criticality cont.

- To relate  $k_p$  and  $k_{\text{eff}}$ , the fraction of delayed neutrons in comparison to the overall population needs to be defined.
- The delayed neutron fraction is  $\beta$ .
- Energy difference between prompt and delayed neutrons means they have different probability to induce fission.
- To correct for this, an effective neutron fraction is created,  $\beta_{\text{eff}}$ .
- At prompt  $k_{\text{eff}} \approx 1 + \beta_{\text{eff}}$ .

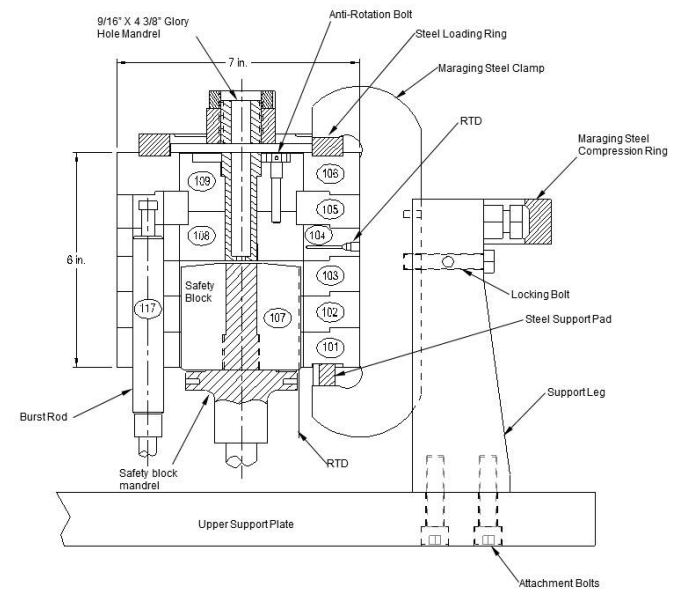
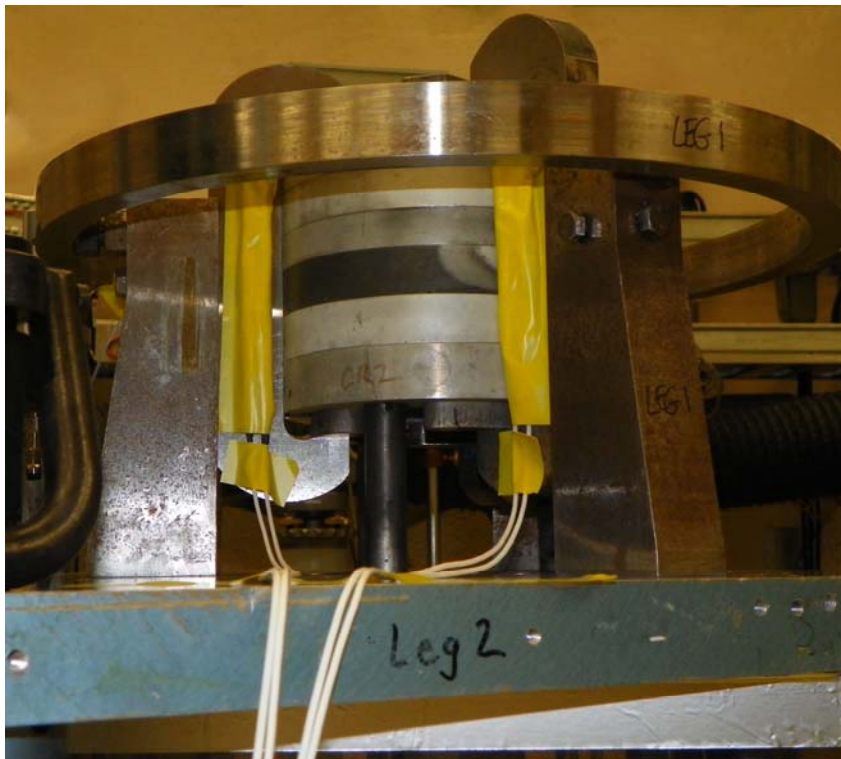
# Experiment – Critical Assemblies

## Godiva IV

- **Fast metal critical assembly.**
- **Designed for fast burst operations.**
- **Fuel is about the size of a coffee can. (7 in. diameter, 6 in. height)**
- **65 kg of 93.5% enriched  $^{235}\text{U}$ .**
- **Control elements are  $^{235}\text{U}$  and control the amount of mass to adjust reactivity.**
  - Three reactivity control elements
    - One Safety Block (coarse control)
    - Two Control Rods (fine control)
  - One pneumatic “burst rod”



# Experiment – Critical Assemblies cont.



# Experiment – Critical Assemblies cont.

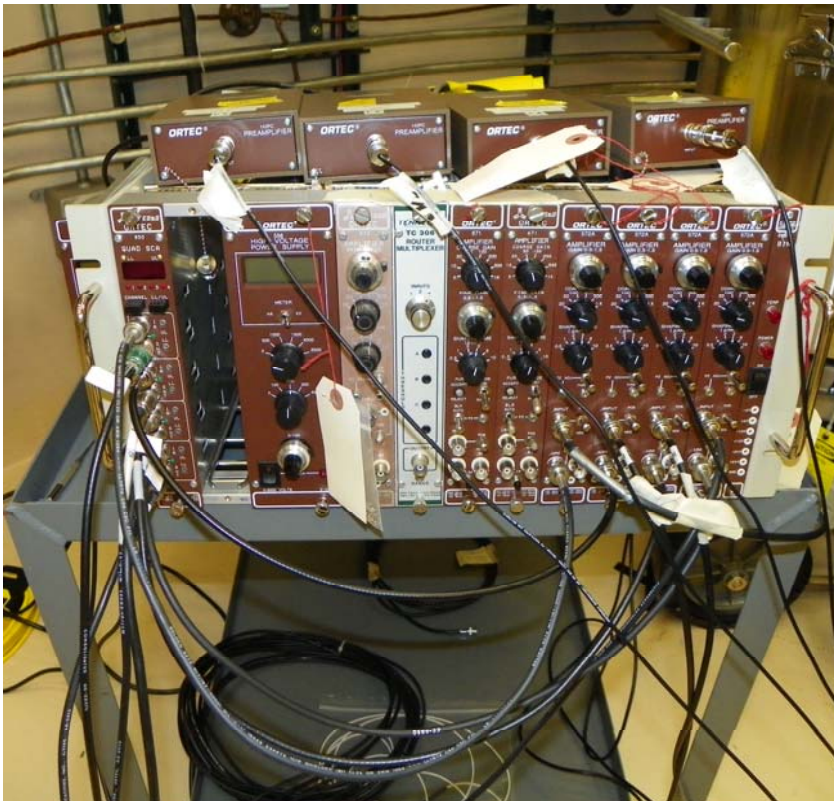
## 13 Foil Configuration

6		1"
4B Poly		1"
4C Poly		1"
2G Poly	18C HEU	0.5"
2E Poly	19C HEU	0.5"
2C Poly	20C HEU	0.5"
2I Poly	13C HEU	0.5"
2J Poly	14C HEU	0.5"
10 RTD	15C HEU	0.5"
Rossi Alpha Plate	16C HEU	0.5"
3 Membrane Poly	17C HEU	0.5"
2K Poly	21C HEU	0.5"
2L Poly	22C HEU	0.5"
2F Poly	23C HEU	0.5"
2D Poly	24C HEU	0.5"
9 Poly Source	25C HEU	0.5"
11 Poly		0.5"
4A Poly		1"
5 Poly		1"

## 10 Foil Configuration

6		1"
4B Poly		1"
4C Poly		1"
2E Poly	16C HEU	0.5"
2C Poly	17C HEU	0.5"
2I Poly	18C HEU	0.5"
2J Poly	19C HEU	0.5"
2K Poly	20C HEU	0.5"
Rossi Alpha Plate	21C HEU	0.5"
2L Poly	22C HEU	0.5"
2F Poly	23C HEU	0.5"
2D Poly	24C HEU	0.5"
9 Poly Source	25C HEU	0.5"
11 Poly		0.5"
4A Poly		1"
5 Poly		1"

# Experiment – Neutron Detection System cont.



## Experiment – Neutron Sources

- **Two different sources used during these measurements.**
  - DT generator
    - 14 MeV neutrons
    - 50 Hz
    - $10^6$  neutrons per pulse
  - $^{252}\text{Cf}$  source
    - Spontaneous fission source
    - $10^5$  neutrons per second

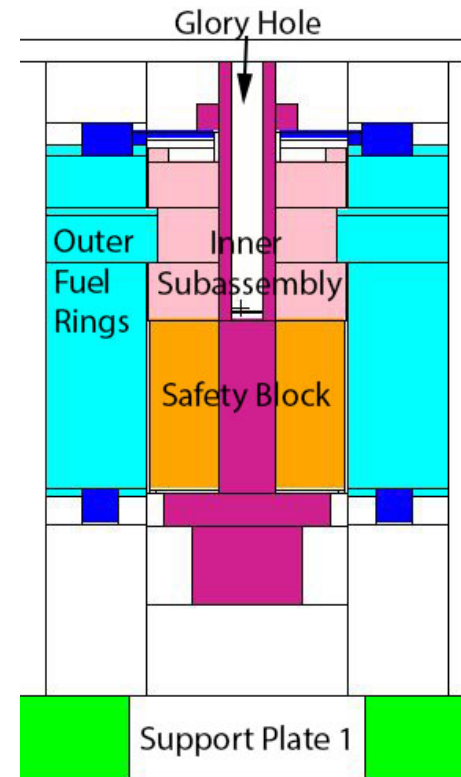


## Experiment – Execution

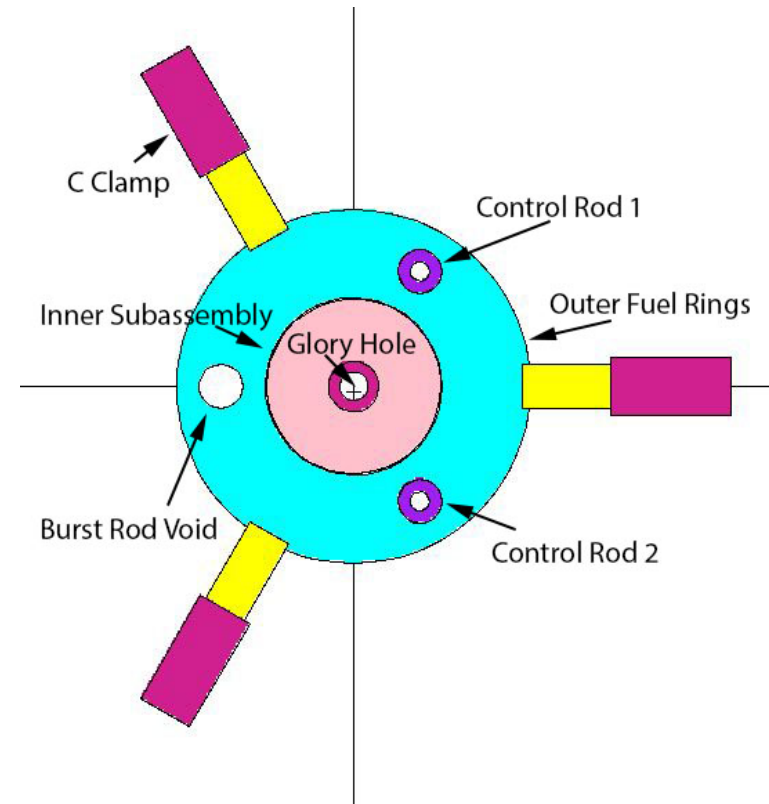
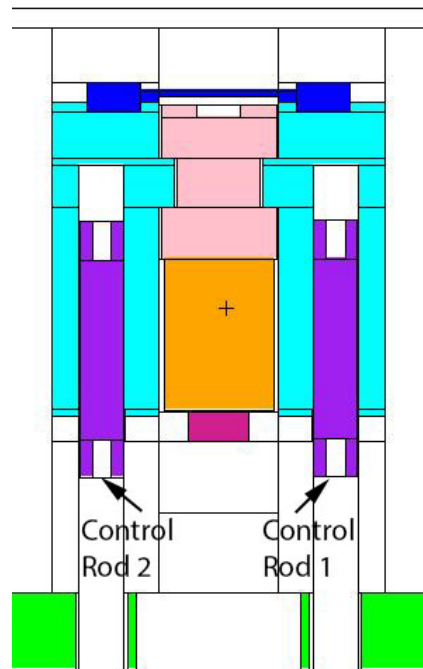
- **The Rossi- $\alpha$  Method utilizes time correlations between neutron detection events to derive the time constant of a chain reacting system.**
- **Measurements executed using a neutron source(s).**
  - Godiva IV – DT source placed on far side of fuel with respect to the detectors.
  - Polyethylene Class Foils- Cf-252 Source placed in bottommost unit of each configuration.
- **List-mode data was collected on steady-state neutron populations of various configurations.**
  - Godiva IV – 50, 100, 150 cents subcritical.
  - Polyethylene Class Foils – 15, 14, 13, 12, 11, 10, and 5 units.
    - Measurements also completed as a function of separation from critical at 34, 63, and 94 mils w/ foils.
    - Not used for reactivity study because of potential variability in the positioning.

## Calculation – Godiva IV

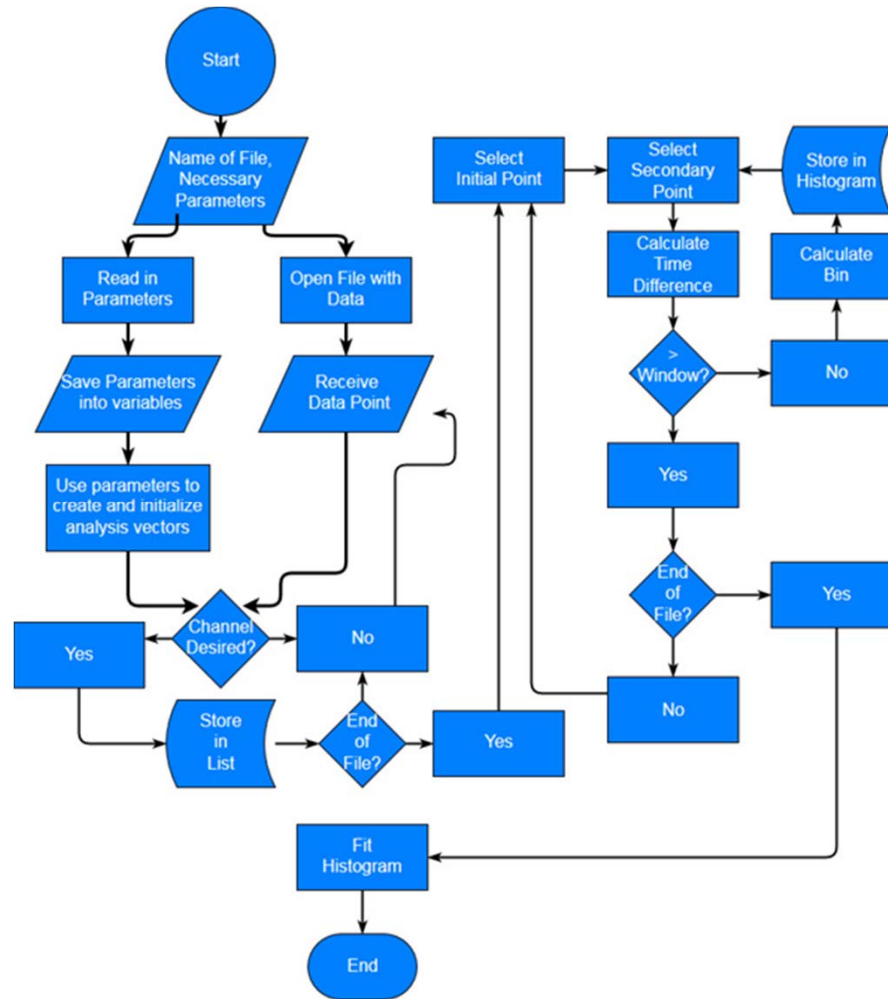
- **Benchmark model of Godiva IV was updated.**
- **Control rods in this model were moved in 100 mil increments for the full range of travel.**
- **The safety block was moved in 500 mil increments covering the full range of travel.**
- **Because no experimental results were obtained, only the definition of  $\alpha$  method was used.**



# Calculation – Godiva IV cont.

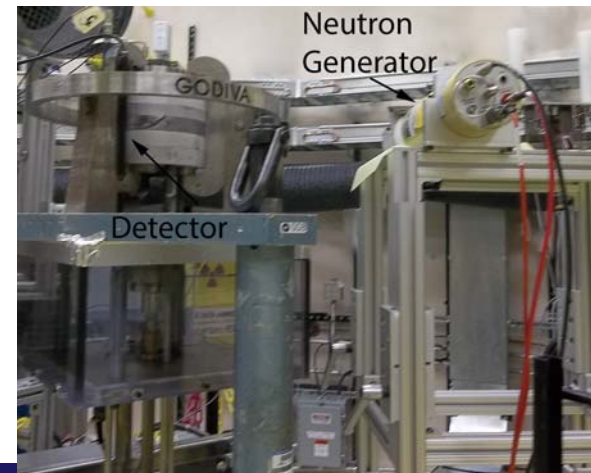


# Analysis – Algorithm



## Results – Godiva IV

- **Results were not obtained from the measurements taken.**
- **Decay constants were so fast that significant portion of the decay was within the system dead time.**
- **Faster detection system will be required to perform measurements on a system with decay constants as fast as Godiva IV.**
  - Rather than obtain a fast detection system and perform validation on it, a slower system was measured.
- **Simulation results are given for the definition of  $\alpha$  method as these were performed in a preliminary capacity.**
- **Additionally, Godiva IV may not have a large enough range of reactivity to perform these measurements.**



## Analysis – Statistical Uncertainty

- In an ideal world, a large number of measurements of each configuration would have been completed.
- In reality, 10 measurements were performed on each configuration except the 5 foil case for the Polyethylene Class Foils.
- This is not a large number.
- For the purposes of quantifying the statistical uncertainty on the measurements, the standard deviation was taken on this small population.
- Was ~2% for each case.
  - Very good.
  - Slightly higher on the 12 foil case.
    - Unintentional ARO during measurement.

## Results – Polyethylene Class Foils cont.

- **The systematic uncertainty for the system was then determined using the perturbed parameters previously discussed.**
  - Position of detectors in the plate.
  - HEU mass
  - Polyethylene plate mass
  - Polyethylene plate dimensions
  - Axial air gap
- **Of these parameters, the uncertainty on HEU mass had the largest impact on the total uncertainty.**
- **Leads to what seems like a rather large uncertainty for the first couple data points.**
- **To reduce this uncertainty, the foils would need to be weighed on a more sensitive scale such that the standard uncertainty in the parameter can be reduced.**

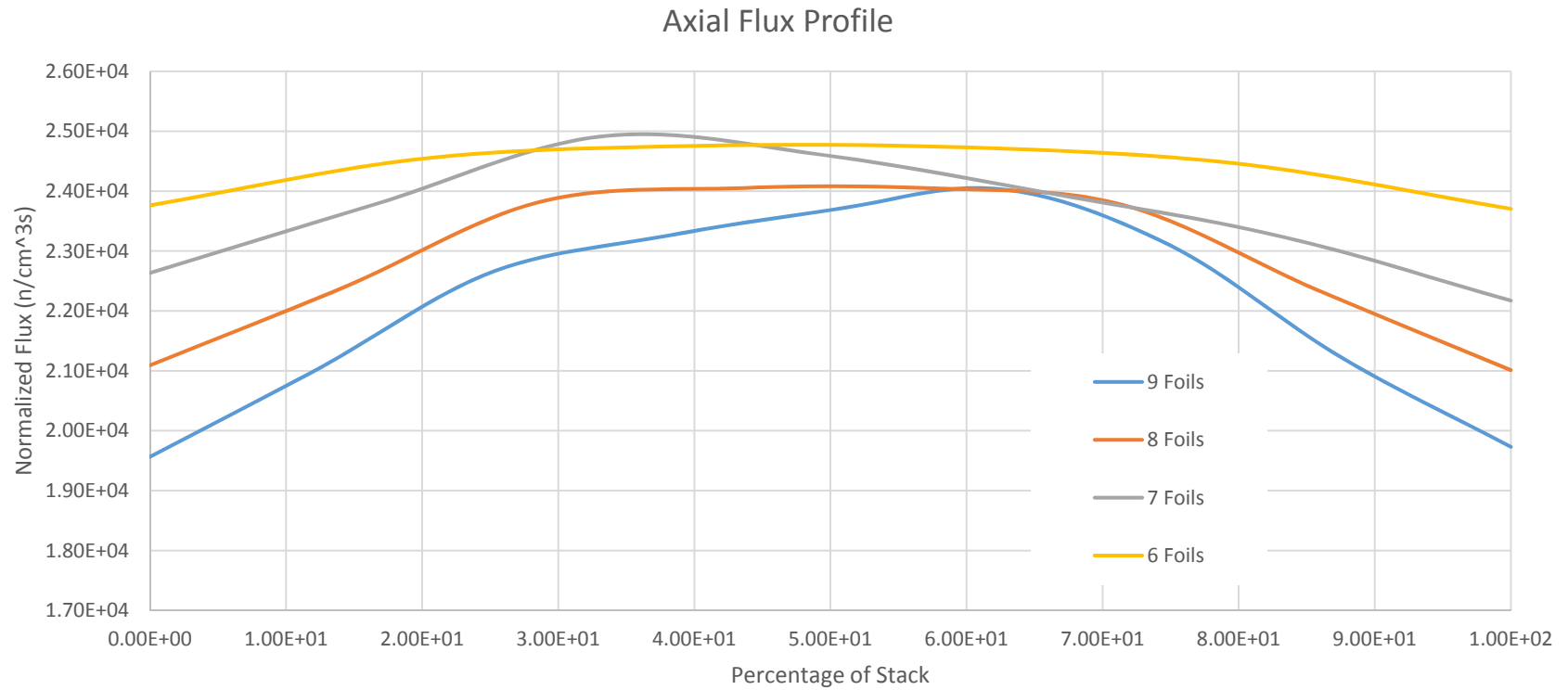
# Separability

$$\frac{1}{v} \frac{\partial \phi}{\partial t} + \Omega \cdot \nabla \cdot \phi + \sigma \phi = q$$
$$\phi(r, \Omega, E, t) = e^{\alpha t} \phi(r, \Omega, E)$$

## Results – Polyethylene Class Foils cont.

- A study was also completed examining the axial flux profile to determine if shape changes in the flux profile could indicate a breakdown of the separability of the spatial and temporal flux distributions.
- It was found that in an integral sense (typical flux tallies) there is no indication of this behavior.
- Suppressions in the flux shown in the graph on the next page due to the detection system remove perfect symmetry from the distribution.

# Results – Polyethylene Class Foils cont.



# Expected Flux Profiles

